ADAPTIVE DIGITAL PREDISTORTION FOR POWER AMPLIFIER LINEARIZATION

A THESIS

SUBMITTED TO THE DEPARTMENT OF ELECTRICAL AND

ELECTRONICS ENGINEERING

AND THE INSTITUTE OF ENGINEERING AND SCIENCE

OF BILKENT UNIVERSITY

IN PARTIAL FULFILLMENT OF THE REQUIREMENTS

FOR THE DEGREE OF

MASTER OF SCIENCE

By

Makbule Pehlivan Aslan

December 2008

I certify that I have read this thesis and that in my opinion it is fully adequate, in scope and in quality, as a thesis for the degree of Master of Science.

Prof. Dr. Abdullah Atalar(Advisor)

I certify that I have read this thesis and that in my opinion it is fully adequate, in scope and in quality, as a thesis for the degree of Master of Science.

Dr. Tarık Reyhan

I certify that I have read this thesis and that in my opinion it is fully adequate, in scope and in quality, as a thesis for the degree of Master of Science.

Assist. Prof. Dr. F. Ömer İlday

Approved for the Institute of Engineering and Science:

Prof. Dr. Mehmet B. Baray
Director of the Institute

ABSTRACT

ADAPTIVE DIGITAL PREDISTORTION FOR POWER AMPLIFIER LINEARIZATION

Makbule Pehlivan Aslan
M.S. in Electrical and Electronics Engineering
Supervisor: Prof. Dr. Abdullah Atalar
December 2008

High power amplification of linear modulation schemes which exhibit fluctuating envelopes, invariably leads to the generation of distortion and intermodulation products. In order to avoid these effects, maintaining both power and spectral efficiency, it is necessary to use linearization techniques. By using linearization techniques, the amplifier can be operated near the saturation with good efficiency and linearity.

The technique proposed here is predistortion based on a look-up table (LUT) method using input and output signal envelopes. The predistortion is implemented using a LUT and an address generation block that selects the appropriate coefficient from the LUT, given the magnitude of the input signal. The testing of the predistorter is done by using a baseband system model which consists of a 16-QAM modulator, an upsampler, a raised cosine filter, the predistorter and a baseband behavioural amplifier model. The performance of the predistorter with a new LUT update method is evaluated in terms of power efficiency and spectrum efficiency. MATLAB simulations show that to obtain up to 25-30 dB improvement in power spectrum is possible and sufficiently large LUT size is needed to reduce the background noise level. Furthermore, the performance of the predistorter in the case of an amplifier with memory is also investigated.

The algorithms have been implemented on an FPGA chip. The performance of the system is as predicted in MATLAB simulations.

Keywords: adaptive digital predistortion, look-up table predistortion, linearization, amplifier nonlinearity, spectrum efficiency, FPGA.

ÖZET

UYARLANABİLİR SAYISAL ÖNBOZMA KULLANILARAK GÜÇ KUVVETLENDİRİCİLERİNİN DOĞRUSALLAŞTIRILMASI

Makbule Pehlivan Aslan
Elektrik ve Elektronik Mühendisliği, Yüksek Lisans
Tez Yöneticisi: Prof. Dr. Abdullah Atalar
Aralık 2008

Dalgalanan zarf gösteren doğrusal modülasyon şemalarının güç yükseltilmeleri kaçınılmaz olarak bozulma ve aramodülasyon ürünlerine sebep olur. Bu etkilerden kaçınmak, gücü ve spektral verimi devam ettirmek için doğrusallaştırma teknikleri kullanılmalıdır. Doğrusallaştırma teknikleri kullanılarak, yükseltici doyma noktasına yakın yerlerde iyi verim ve doğrusallıkla çalıştırılabilinir. Bu tezde giriş ve çıkış sinyal zarfları kullanılarak güncellenen tablo temelli sayısal önbozma yöntemi sunulmaktadır. Ön bozma yöntemi, giriş sinyalinin büyüklüğü verildiğinde güncelleme tablosundan uygun adresten doğru katsayıyı seçen bir adres oluşturma bloğu ile gerçekleştirilmiştir. Ön bozma algoritması 16'lık dördün genlik kipleyici, yukarı örnekleyici, filtre, ön bozma bloğu ve temelbant karakterli güç yükselticisinden oluşan bir temelbant sistem modeliyle test edilmiştir. Yeni bir tablo güncelleme metoduna dayanan ön bozma algoritması güç ve spektrum verimi açısıdan değerlendirilmiştir. Algoritma kullanılarak güç spektrumunda 25-30 dB iyileşme sağlanabileceği ve büyük tablo boyutları kullanılarak bant dışı gürültü seviyesinin azaltılabileceği gösterilmiştir. Ek olarak, ön bozma algoritmasının yükselticinin hafızalı olması durumundaki performansı incelenmiştir. Algoritma bir FPGA çipi ile denenmiş ve performansının MATLAB simulasyonlarıyla uyuştuğu gözlemlenmiştir.

Anahtar sözcükler: uyarlanabilir sayısal önbozma, taramalı tablo temelli ön bozma, doğrusallaştırma, amplifikatör doğrusalsızlığı, spektrum verimi, FPGA..

Acknowledgement

First and foremost, I gratefully thank my supervisor Prof. Abdullah Atalar for his suggestions, supervision, and guidance throughout the development of this thesis. I feel very fortunate for the opportunity to have him as my research advisor.

I would also like to thank Dr. Tarık Reyhan and Assist. Prof. Dr. F. Ömer İlday, the members of my jury, for reading and commenting on the thesis.

I would like to express my special thanks to Burak Şekerlisoy and Oğuzhan Atak for their effort that they provided during the implementation part of my M.S. study and for their friendship.

I would like to thank my beloved husband Furkan with deepest appreciation for his incessant encouragement and motivation.

I would also like to thank my parents and my brother for their love and support that they gave me all my life.

I would like to thank Özlem Yılmaz, İmran Akça, Akın Avcı and Rohat Melik for their valuable friendship.

Finally, I would like to thank The Scientific and Technological Research Council of Turkey (TÜBİTAK) for the financial support provided during my M.S. study.

Contents

List of Figures

To My Furkan and My Family ...

Chapter 1

INTRODUCTION

1.1 Background

The recent trend in modern information technology has been towards the increased use of portable and handheld devices such as cellular telephones, personal digital assistants (PDAs), and wireless networks. This trend presents the need for compact and power efficient radio systems. Typically, the most power consuming device in a radio system is the power amplifier (PA). Therefore, radio frequency power amplifiers (PAs) represent the most critical and costly component in wireless communication systems today. To be able to accurately decode most modern digitally modulated signals, linear amplification and frequency conversion are necessary throughout the transmit and receive portions of the system. Any amplitude and/or phase distortions on the signal may reduce the ability to decode these signals properly. Due to the limited amount of available frequency spectrum, communication channels are quickly becoming crowded. Therefore it is also necessary to find new and innovative ways to reach these limits and possibly push them even further. This push towards increased bandwidth usage presents a need for increased bandwidth efficiency in order to increase system capacities. The current solution is found in more bandwidth efficient modulation schemes, which in turn requires highly linear amplification throughout radio architectures.

Modulation types such as QAM exhibit greatly improved bandwidth efficiency at the expense of further susceptibility to nonlinearities due to their large non-constant envelope [6], [22]. This type of modulation techniques that are used to transmit large amount of data introduce amplitude (AM/AM distortion) and phase (AM/PM distortion) distortions to the input signal due to their highly varying envelopes. This distortion problem can be solved by a linear amplifier. But, several problems arise when the designer requires a linear amplifier in a radio system. The first major problem is that linear amplifiers are generally very inefficient in their use of power. The second major problem with the use of linear amplifiers is the cost factor. Typically, a high efficiency, saturating amplifier is simply backed-off from the compression point to an input power point that exhibits the required linearity. This back-off method is quite acceptable and is used widely in industry; however, the cost associated with doing this is high since the designer is using a more expensive, higher power amplifier to do the job. The higher power amplifier must be operated at a lower power output, which could result in a low efficiency and high power dissipation. This problem is solved by linearization techniques. By applying linearization to the power amplifier, the linearity is improved, the required backoff is decreased and therefore the efficiency is increased. The idea of linearization is that the power amplifier itself is designed to be not linear enough in order to achieve good efficiency, after which the linearity requirements are fulfilled by external linearization.

1.2 Thesis Objective and Outline

Power amplifier linearization techniques can be divided into 3 main groups feedback, feedforward and predistortion. Recently, predistortion is the most commonly used linearization technique. The aim in the predistortion method is to introduce inverse nonlinearity before the nonlinear power amplifier that can compensate the AM/AM and AM/PM distortions generated by the amplifier. The most commonly used form of predistortion method is digital baseband predistortion. In order to compensate the characteristic changes of the power amplifier, the adaptivity of the predistortion method is very important and preferred. In

this thesis, a complex gain-based look-up table predistorter is implemented and tested both in software and in hardware. The outline of the thesis is as follows: Chapter 2 represents the power amplifier linearization techniques study. Chapter 3 introduces effects of power amplifier nonlinearity and memory in communications systems. Chapter 4 describes the implementation of the proposed complex gain-based look-up table predistorter in software. Chapter 5 represents the response analysis the of the proposed predistortion method. Chapter 6 represents the System Generator and FPGA implementations. Finally, Chapter 7 gives the conclusion and presents possible future work.

Chapter 2

POWER AMPLIFIER LINEARIZATION TECHNIQUES STUDY

As it is mentioned in Chapter 1, to obtain both linear amplification and high power efficiency, a linearizer is required. The linearizer allows the amplifier to be operated at much higher operating point since the distortion generated by the amplifier because of the peaks in input signals can be corrected up to the saturation level of the amplifier as shown in Figure 2.1. Any input signal which drives the amplifier to hard saturation, the resulting distortions cannot be corrected since any increase in input power beyond this point will not result in an increase in output power.

A wide range of linearization techniques is available to the modern power amplifier/ communication system designer. These techniques can be roughly classified into three groups: (1) Feedback, (2) Feedforward, and (3) Predistortion. Each of these three groups contains several techniques. These techniques will be briefly described in the following sections.

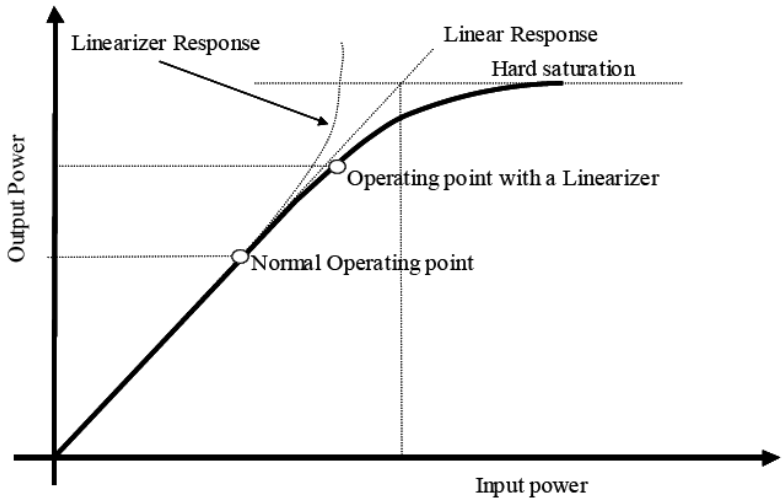

Figure 2.1: Performance Improvement of a Power Amplifier with a Linearizer

2.1 Feedback

The simplest method of reducing amplifier distortion is by some form of feedback. Feedback is used extensively in audio amplifiers and in automatic plant control but it can also be used to linearize power amplifiers [14]. The Figure 2.2 illustrates the use of negative feedback around an amplifier with the effect of distortion n(t). G is the gain of the amplifier and K is the feedback attenuation.

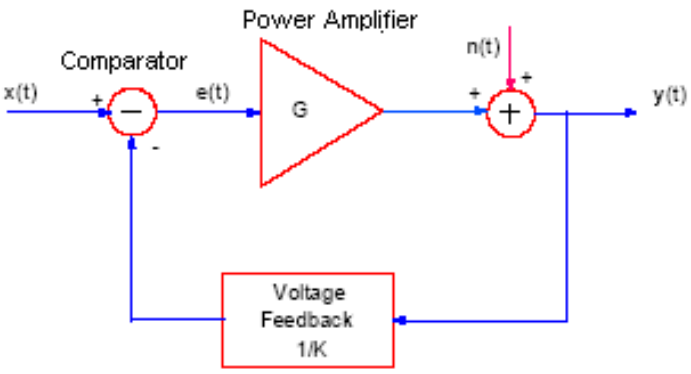

Figure 2.2: Simple Feedback to Linearize Power Amplifiers

$$\textbf{Output: } \mathbf{y(t) = G \times e(t) + n(t)} \tag{2.1}$$

$$\textbf{Feedback: } \mathbf{f(t) = y(t)/K} \tag{2.2}$$

$$\textbf{Error: } \mathbf{e(t) = x(t) - f(t)} \tag{2.3}$$

Therefore,

$$\mathbf{y(t) = K \times (G*x(t) + n(t))/(G+K)} \tag{2.4}$$

If the amplifier gain is much greater than the feedback ratio $G \gg K$, then $K + G$ approximates to G. So

$$\mathbf{y(t) = K \times x(t) + (K \times n(t))/G} \tag{2.5}$$

Therefore, the distortion produced by the main amplifier is reduced by a factor K/G. The disadvantage of this approach is that the improvement in distortion performance is at the expense of the gain of the power amplifier and also feedback needs more bandwidth than signal.

2.1.1 Envelope Feedback

Simple envelope feedback has matched envelope detectors coupled to the power amplifiers input and output ports. A differential amplifier forms amplitude error-correcting amplifier based on the detected envelope signals. The resulting error is used to control the gain of the amplifier. This technique has been widely employed to improve the IMD performance of VHF and UHF solid-state power amplifiers in the mobile communication industry. The main draw back is that since this technique performs simple amplitude correction, it starts generation IMD products when the envelope operates in the compression region of the amplifier. The delays in the detection and signal processing can cause phase differences between AM and PM processes. This may cause asymmetry IM side bands and may substantially reduce any correction obtained by amplitude feedback process [1].

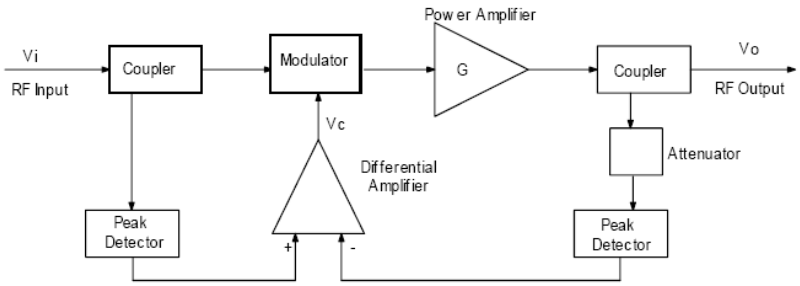

Figure 2.3: Envelope Feedback to Linearize Power Amplifier
[1]

2.1.2 Polar Feedback

The polar feedback technique combines the envelope feedback with an additional feedback loop to account for phase shift variation through the power amplifier by dynamically adjusting the phase of the Radio Frequency (RF) input. The phase correction shown in Figure 2.4 uses a phased locked loop to maintain a constant phase shift over the amplifiers dynamic range. The two feedback loops are interdependent, any variation in the AM/AM loop, will produce phase as well as gain variation and similarly AM/PM will interact with the AM/AM loop if the insertion loss of the phase shifter varies. It has been reported in the literature that phase amplifier requires much higher bandwidth, which is a major limiting factor in the performance of the polar feedback [20].

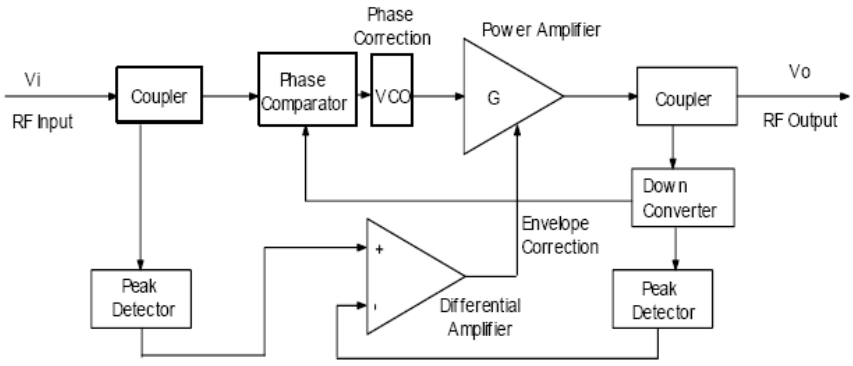

Figure 2.4: Polar Feedback to Linearize Power Amplifier
[20]

2.1.3 Cartesian Feedback

The cartesian feedback is similar to polar feedback described previously, however, the baseband signal information is processed in I and Q form. Therefore the I and Q channels are well matched, eliminating the problems of different bandwidth and processing requirements for magnitude and phase paths as in polar feedback.

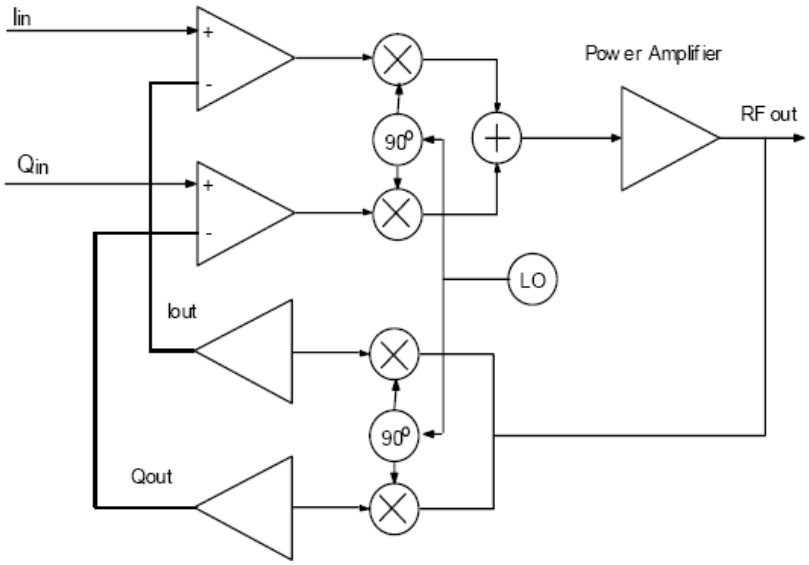

Figure 2.5: Cartesian Feedback to Linearize Power Amplifier [15]

Figure 2.5 shows the cartesian feedback loop. The input signal is separated into I and Q and fed to differential amplifier where input signals is subtracted from the feedback signal. The error signal is upconverted to RF using a local oscillator and then combined to produce the complex RF, which is amplified by the power amplifier. The output of the power amplifier is sampled using a directional coupler and down converted and separated into I and Q using the same local oscillator used in up conversion process. The down convert output forms the feedback to the differential amplifiers. A phase shift network is required to ensure that the up and down conversion processes are correctly synchronized. The main advantages of cartesian over polar feedback is that a significant reduction in bandwidth requirement for the feedback loop allows more reduction of IMD and secondly simplicity of implementation. The experimental results in the literature

have shown that 10-30 dB of improvement in IMD performance is achievable, however the stability criteria limits the maximum bandwidth to a few megahertz [10][2].

2.2 Feedforward

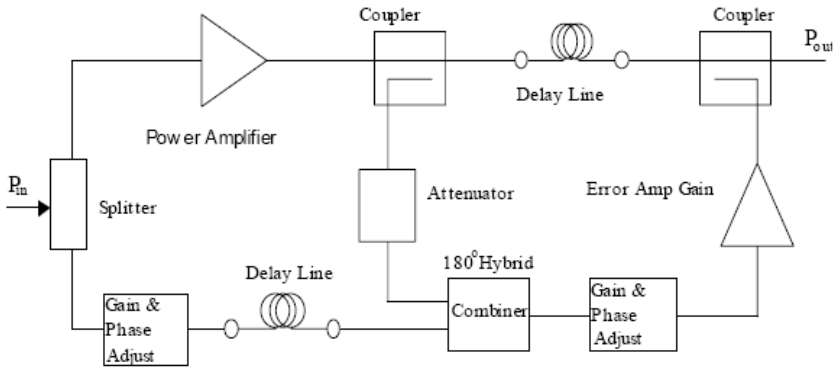

Figure 2.6: Feedforward Technique to Linearize Power Amplifier [12]

As shown in Figure 2.6, in the feedforward system the power amplifier is fed directly with the RF source signal. The delayed sample of the undistorted input RF signal is compared with an attenuated sample of the power amplifier output. The error signal is then amplified linearly to the required level and is recombined with the output, following a delay line in the main signal path, which compensates for the delay in the error amplifier. The error signal cancels the distortion present in the main path leaving an amplified version of the original signal. The distortion generated by the power amplifier is cancelled in the feedforward loop by subtracting the source signal from the power amplifier output. The resulting error signal is subtracted from the amplifier output RF components. Additionally, it does not require a phase-locked loop to maintain phase correction. The advantage of feedforward technique is that the bandwidth is determined by frequency response of the couplers, delay lines, and phase shift components, which can be made to be very stable over a wide operating range. The disadvantage is the need for error amplifier which will be of a similar size as the main amplifier

[12]. In theory the feedforward loops can be nested as many times as necessary to obtain required level of correction. This method is called multi-stage feedforward. However this method adds cost, complexity, weight and high power dissipation.

2.3 Envelope Elimination and Restoration

The Envelope Elimination and Restoration (EER) technique to linearize the power amplifier was first proposed by Khan [13] to improve short-wave broadcast transmitter. The EER has an envelope detector, which extracts the magnitude information and limiter, which eliminates RF envelope and generates a constant amplitude phase signal (See Figure 2.7). The magnitude and phase signal are amplified, with the delay path of two signal matched. The magnitude and phase are then recombined using switch-mode power amplifier. The experimental results have shown that EER provides greater than 28 dB of linear output power with 33-49% efficiency[24].

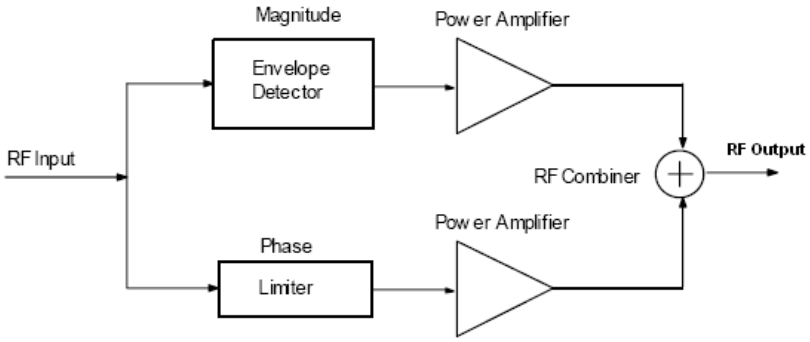

Figure 2.7: EER Technique to Linearize the Power Amplifier [24]

It is also possible to introduce feedback to envelope elimination and restoration technique. The feedback introduced EER can be seen in the literature in [24] and [21]. However the proposed feedback method causes stability problems and increases the complexity of the system.

2.4 Linear amplification with Nonlinear Components (LINC)

Linear amplification with Nonlinear Components (LINC) is, different from all other techniques of linearization of power amplifier, because no feedback from the output of the power amplifier is used. The power amplifier can be highly non linear. The theory of operation is that the baseband processing accepts a gain and phase modulated input signal, and generate two wideband constant envelope phase modulated signals. These signals are up-converted through two well matched non linear amplifier chains and summed [11]. The complex signals are generated such that all undesired out-of-band components are in exact anti-phase in the two amplifier chains and cancel at the output, while the wanted components are in phase and reinforced (Figure 2.8).

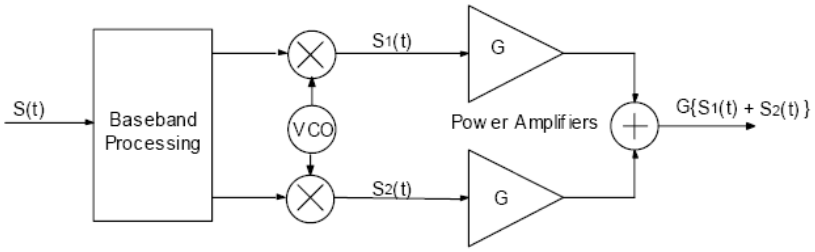

Figure 2.8: LINC method to Linearize Power Amplifiers [11]

The generation of two wideband constant envelope phase modulated signals $S_1(t)$ and $S_2(t)$ have to be accurate. The DSP technology allows $S_1(t)$ and $S_2(t)$ to be generated more accurately. Thus, the linearity performance of the technique is determined by the gain and phase match between the two amplifiers [26] [8]. The input signal $S(t)$ is complex representation of bandlimited signal and can be written as

$$\mathbf{S(t) = a(t) * e^{j\phi(t)}; 0 < a(t) < a_{max}} \tag{2.6}$$

This signal can be split into two signals, $S_1(t)$ and $S_2(t)$, with modulated phase and constant amplitudes as described in [8]. This gives:

$$S_1(t) = S(t) - e(t); S_2(t) = S(t) + e(t); and |S_1(t)| = |S_2(t)| = a_{max}; \tag{2.7}$$

Where e(t) is in quadrature to the source signals $S_1(t)$ and $S_2(t)$,

$$e(t) = j \times S(t) \times \sqrt{(\frac{{a_{max}}^2}{|S(t)|^2} - 1)}; \tag{2.8}$$

The output is given by:

$$\mathbf{S}_{out}\mathbf{(t)} = \mathbf{2GS(t)}; \tag{2.9}$$

The quadrature signal e(t) is added to one leg of forward loop and subtracted from the other leg of forward loop to give a constant envelope signal. The main disadvantage with this approach is that the characteristics of the two power amplifiers used should be as identical as possible. Another problem with LINC is the bandwidth occupied by the separated signal components $S_1(t)$ and $S_2(t)$ can be 10 or more times larger than the original bandwidth [14].

2.5 Combined Analog-Locked Loop Universal Modulator (CALLUM)

The Combined Analog Locked Loop Universal Modulator (CALLUM) is similar to the LINC technique where it combines two constant amplitude signals to form the output signal [25]. CALLUM has two Voltage Controlled Oscillators (VCO) which generate separate phase modulated vectors of amplitude S and phase ϕ_1 and ϕ_2 as shown in Figure 2.9. The addition of these two vectors results in gain and phase modulated output vector [5]. The main problem of CALLUM is stability which limits its use to narrowband applications.

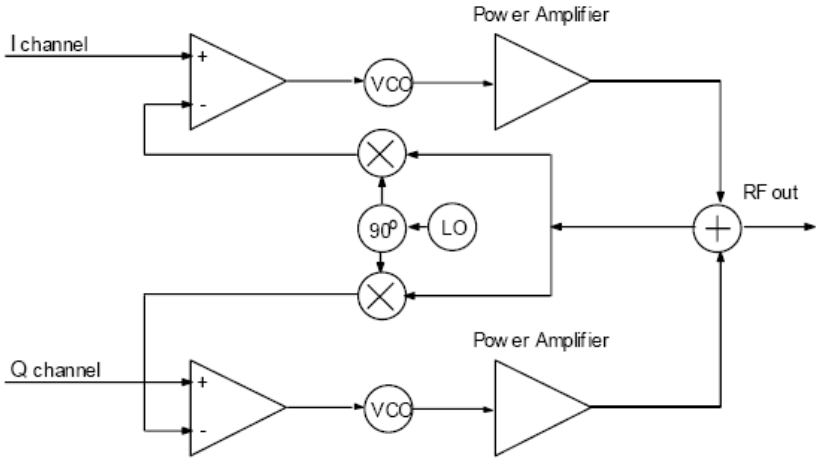

Figure 2.9: CALLUM Feedback to Linearize Power Amplifier [5]

2.6 Predistortion

Predistortion is one of the major linearization techniques. The literature search shows that from all the linearization techniques that have been developed, the predistortion is the most commonly used in the new systems today. The main idea of predistortion technique is to insert a non-linear element called predistorter of preceding the nonlinear power amplifier which has the inverse transfer characteristics of the power amplifier. Figure 2.10 shows predistortion in its simplest form [19]. Therefore, the predistortion technique results in a linear input-output relationship for the predistorter-amplifier combination.

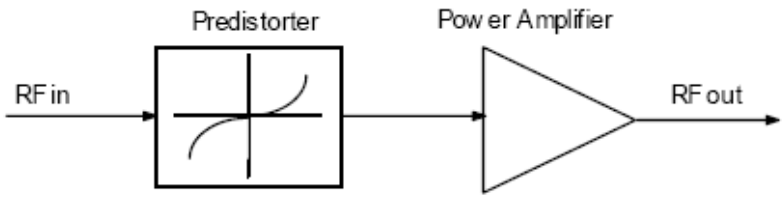

Figure 2.10: Simple Predistortion Technique to Linearize Power Amplifier

Considering the position of the predistorter, predistortion technique can be divided into three main categories: **(1) RF Predistortion, (2) IF predistortion, and (3) Baseband Predistortion**.

In linearization techniques, one of the important critical issue is that the characteristics of the power amplifier can be changed by aging, temperature changes and output load changes. The linearization of the power amplifiers in such a case, can be achieved by providing the predistortion system adaptive. Therefore predistortion techniques can also be divided into two categories: **(1) Adaptive Predistortion, (2)Non- Adaptive Predistortion**. Adaptation algorithms can be applied to each of RF, IF and Baseband predistortion techniques, but it is more commonly applied to baseband predistortion [14]. Therefore *Adaptive Baseband Predistortion* is the most commonly used technique in the new systems today.

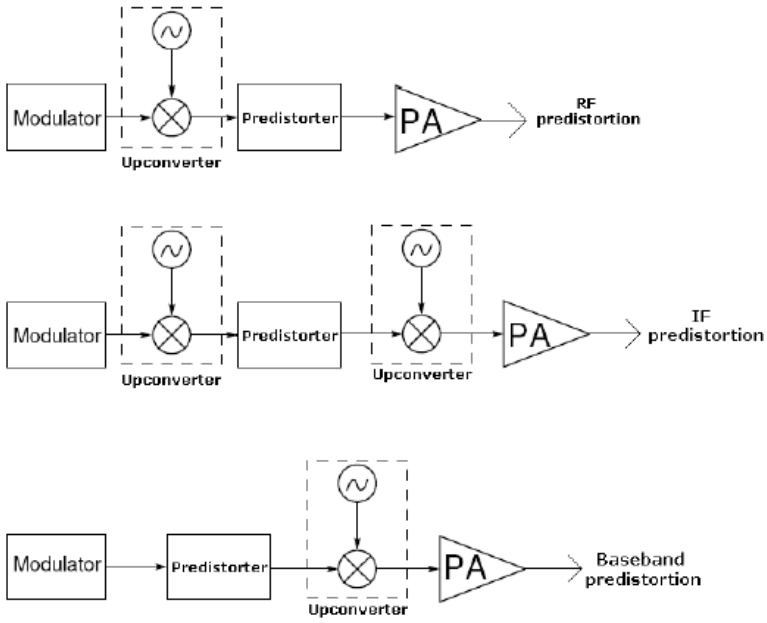

Figure 2.11: RF Predistortion, IF Predistortion, Baseband Predistortion [14]

2.6.1 RF/IF Predistortion

As it is shown in Figure 2.11 the position of the predistorter in the transmission path determines the type of the predistortion. In RF predistortion, the predistorter element operates at the final carrier frequency. In IF predistortion, the predistorter element operates at a convenient intermediate frequency. The advantage of the IF predistortion is that same design can be used for range of carrier frequencies by altering the Local Oscillator (LO) frequency. After predistortion, the signal is upconverted to the final carrier frequency [11]. Since in RF predistortion the predistorter operates at the final carrier frequency, making it adaptive is difficult due to its high frequency of operation [14]. Therefore in RF predistortion the nonlinearity to be cancelled must be known [15]. The advantage of the RF predistorter is its ability to linearize the entire bandwidth of the power amplifier. Because of this, RF/IF predistortion is ideal to use in wideband multicarrier systems such as satellite amplifiers or base-station applications [11]. One famous and widely used configuration of RF/IF predistortion is the RF/IF

cubic predistorter (Figure 2.12).

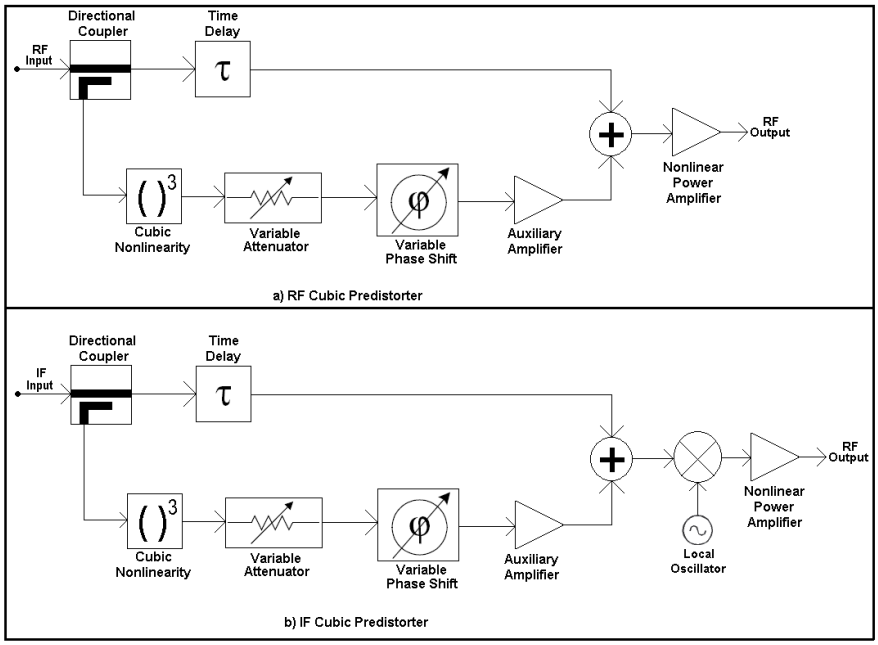

Figure 2.12: (a)RF Cubic Predistorter, (b)IF Cubic Predistorter [14]

It is based on 3rd order intermodulation product cancellation. The input signal is split into two paths. The first path only delays the input signal. The second path has a a cubic (3rd order) nonlinearity, variable phase shifter and attenuator and an auxiliary amplifier. The delay in the first path achieves synchronization between the two paths. The cubic nonlinearity provides a compressive input-output characteristic. The phase shifter and attenuator adjust the phase and amplitude to achieve cancellation of the distortion. The auxiliary amplifier compensates for the significant attenuation introduced by the cubic element. By proper adjustment of the phase, the compressive characteristic provided by the cubic nonlinearity is subtracted from the input signal to obtain an expansive characteristic. This expansive characteristic will compensate for the compressive characteristic of the power amplifier [14]. Several examples of cubic predistorter can be seen in [11].

2.6.2 Baseband Predistortion

In baseband predistortion, predistortion is applied to the baseband signal to be transmitted. In the implementation of baseband predistorters, generally Digital Signal Processors (DSP), FPGAs (Field Programmable Gate Arrays) or ASICs (Application Specific Integrated Circuits) are used. Therefore *baseband predistortion* generally means *digital baseband predistortion.*

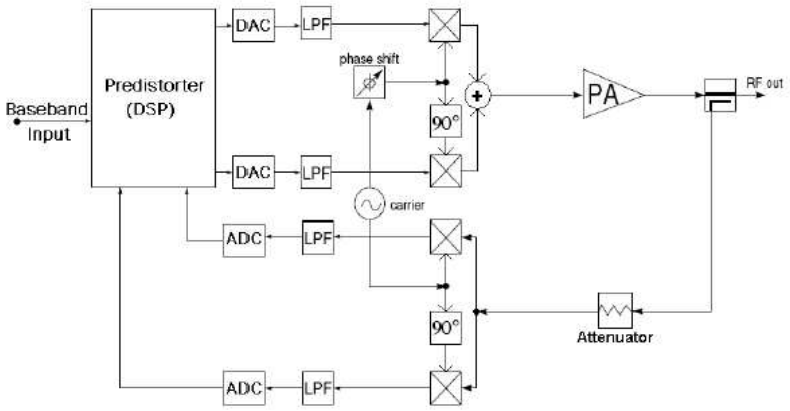

Figure 2.13: Adaptive Digital Baseband Predistortion
[14]

The adaptive version of digital baseband predistortion is called adaptive digital baseband predistortion. Since the proposed predistortion method in this thesis is **Adaptive Digital Predistortion**, this method will be examined in detail. As it is depicted in Figure 2.13, the predistorter distorts the modulated signal. The output of the predistorter is converted to analog form by using D/A converters. The resulting signal is modulated onto the RF carrier and then amplified by the power amplifier. The power amplifier output is sampled, demodulated back into baseband, converted to digital form by using A/D converters and used to adapt the predistorter characteristic [14]. Digital baseband predistorters can be categorized by some operational criteria.

2.6.2.1 Baseband Predistortion According to the Position of the Predistorter

Signal Predistorters: Signal Predistorters apply predistortion after the modulation of the signal. They are generally modulation independent, but their adaptation is slow [14].

Data Predistorters: Data Predistorters operate to compensate the distortion of the constellation diagram. They are generally modulation dependent, their adaptation is faster than signal predistorters.

2.6.2.2 Baseband Predistortion According to the Characteristics of the Power Amplifier

Predistorters without memory: The predistortion has no memory, the adaptation algorithm of the predistorter depends only on the current value of the input. Therefore, memoryless predistorters are unsuccessful to compensate for nonlinearity effects of power amplifiers with memory.

Predistorters with memory: The predistortion has memory, the adaptation algorithm of the predistorter depends not only on the current value of the input but also the past values. Therefore, predistorters with memory can compensate for nonlinearity effects of power amplifiers with memory.

2.6.2.3 Baseband Predistortion According to the Characteristics of the Predistortion

LUT (Look-up table) Predistortion: The predistortion characteristics are stored in a LUT. Different adaptation algorithms can be used in such a way that, every entry of the LUT has to be updated and the addressing of the LUT can be based on the amplitude or the power of the input signal.

Parametric Predistorters: The predistortion is implemented as a nonlinear function such as a polynomial, Volterra series, spline etc. During the adaptation of the used algorithm only the parameters of the nonlinear function should be updated.

2.6.2.4 Baseband Predistortion According to the Adaptation of the Predistorter

Direct Predistorter Adaptation:

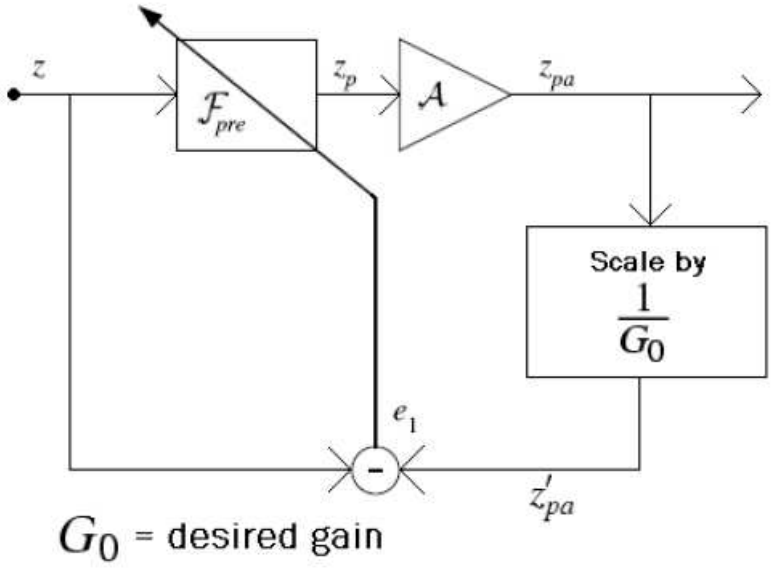

Figure 2.14: Direct Predistorter Adaptation
[14]

The main aim in the direct predistorter adaptation architecture (Figure 2.14), is to adjust predistorter in order to minimize the error between the attenuated output of the amplifier z'_{pa} and the original input signal z. Since A is a nonlinear function, F_{pre} which should be the inverse of A to provide linearity [14] .

Postdistorter Adaptation

The predistortion using postdistorter adaptation (Figure 2.15) is based on the direct identification of the power amplifier inverse using the input and attenuated

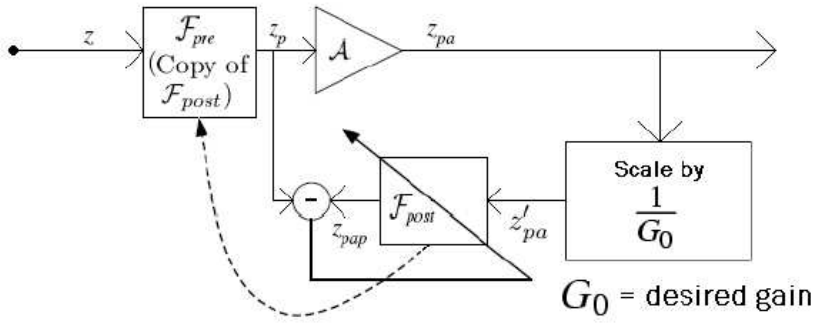

Figure 2.15: Predistortion using Postdistorter Adaptation [14]

output of the power amplifier [14]. For the linearity to be satisfied the optimum solution in the Figure 2.15 is $F_{post}(z)=A^{-1} * (G_0 z)$. F_{post} is obtained by iterative error minimization techniques and since F_{pre} is an exact copy of F_{post}, F_{pre} is also obtained.

Power Amplifier Modeling with Consecutive inverse estimation:

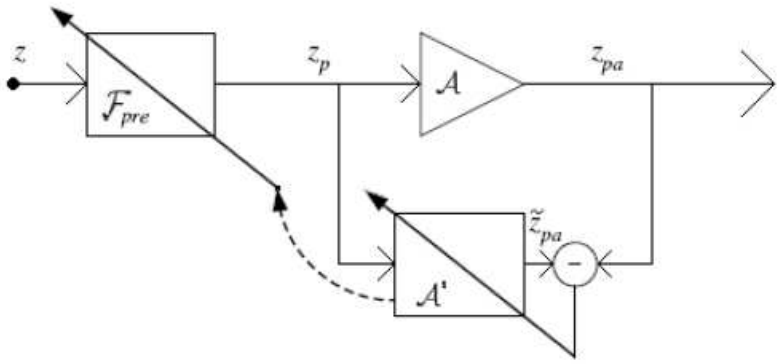

Figure 2.16: PA Modeling with Consecutive Inverse Estimation [14]

Power amplifier modeling with consecutive inverse estimation (Figure 2.16), uses the power amplifier input z_p and output z_{pa} to calculate the power amplifier characteristic estimate A' and then this forward power amplifier model is used to calculate the power amplifier inverse F_{pre} [14].

This thesis proposes a method of LUT predistortion using direct predistorter adaptation. The following section will describe different direct predistorter adaptation algorithms found in the literature for LUT predistorters.

2.6.3 LUT Predistorters with Direct Predistortion Adaptation

The LUT predistorters can be classified as mapping predistorters and gain-based predistorters. Gain-based predistorters can be further classified as polar predistorters and complex gain predistorters.

Complex Gain Based Predistorter:

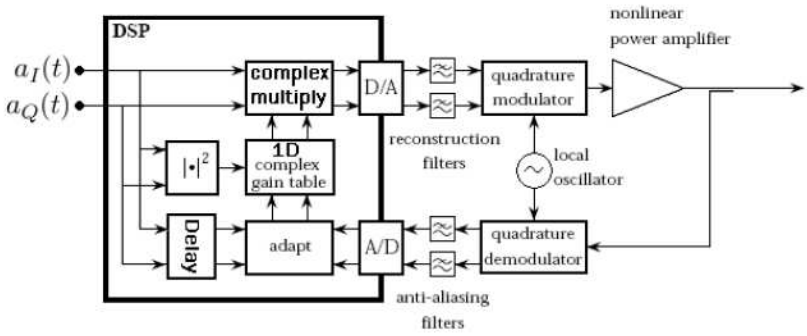

Figure 2.17: Complex Gain Based Predistorter [3]

Complex gain based predistorter shown in Figure 2.17 was proposed in [3] by Cavers. In this method, there is a one dimensional LUT that has entries of complex gain values. The predistortion is obtained by complex multiplication of the input signal and the corresponding predistorter complex gain component. The LUT is addressed by the squared magnitude of the input signal which gives a uniform distribution of the table entries in terms of power [26].

Let $i(n)$ denotes the input signal and $G_{pre}(|i(n)|^2)$ denotes the corresponding predistorter gain component. A denotes the input power dependent complex gain

of the power amplifier and A_0 denotes the desired linear gain. Then, in order the linearity to be satisfied for all input power levels the following equation 2.10 should be satisfied [14].

$$i(n) * G_{pre}(|i(n)|^2) * A(|i(n)|^2 |G_{pre}(|i(n)|^2)|^2) = A_0 * i(n); \tag{2.10}$$

For the above equation to be satisfied entries of the LUT should be adjusted adaptively. There are two different adaptation algorithms explained in [14]. The first one is the secant adaptation algorithm which has LUT update equation of 2.11 and the second one is the successive substitutions adaptation algorithm which has the LUT update equation of 2.12.

$$G_{pre,i}(k+1) = G_{pre,i}(k) + \alpha \frac{e(k)\,(G_{pre,i}(k-1) - G_{pre,i}(k))}{e(k) - e(k-1)} \tag{2.11}$$

where α is iteration constant, k is the iteration index and e(k) is the error signal (the difference between the power amplifier output and the desired output linear output) for k^th iteration of i^th LUT entry [4].

$$G_{pre,i}(k+1) = G_{pre,i}(k)[1 - \mu(\frac{z_{pa}(k) - A_0 z(k)}{z_{pa}(k)})] \tag{2.12}$$

where μ is a convergence constant smaller than 1, $z(k)$ is the input to the predistorter and z_{pa} is the output of the power amplifier.

Polar Predistorter:

Figure 2.18 shows the block diagram of a polar predistorter. As it is seen in the figure, there are two one dimensional LUTs. One of them contains magnitude gain values and the other contains phase rotation values. Polar predistorter differs from complex gain based predistorter since it stores complex gain values in polar form instead of cartesian form.

Similar to complex gain based predistorter the predistortion is obtained by complex multiplication of the input signal and the corresponding predistorter

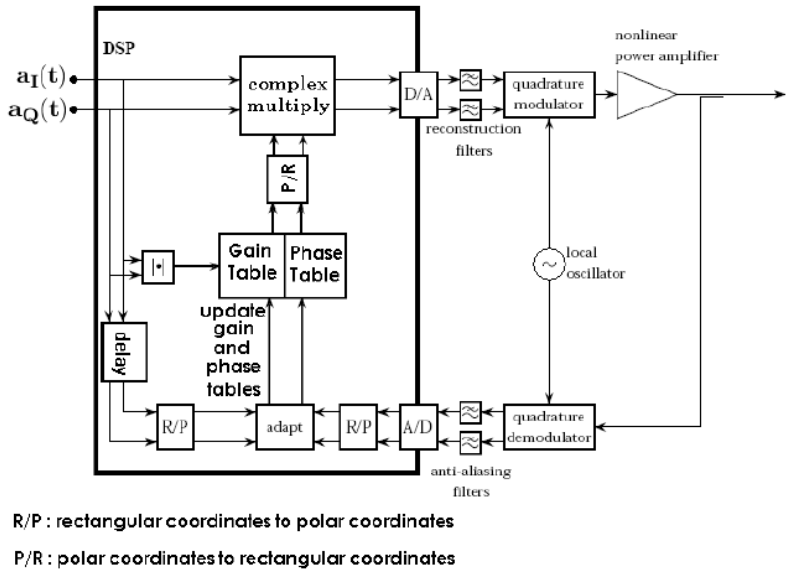

Figure 2.18: Polar Predistorter

complex gain component. In order to apply multiplication it is necessary to convert LUTs entries from polar to rectangular form. Therefore as indicated in the Figure 2.18 it is necessary to use rectangular-to-polar and polar-to-rectangular transformations. This transformations causes complexities in implementation. As in the case of complex gain based predistorter, different adaptation algorithms can be used to update the LUTs. One of the adaptation algorithm found in the literature is the following [9]:

$$G_{pre,i}(k+1) = G_{pre,i}(k) + \mu_g(A_0|z(n)| - |z_{pa}(n)|) \tag{2.13}$$

$$\phi_{pre,i}(k+1) = \phi_{pre,i}(k) + \mu_\phi(arg(z(n)) - arg(z_{pa}(n))) \tag{2.14}$$

where G_{pre} and ϕ_{pre} denote for magnitude gain table characteristic and phase gain table characteristic respectively. A_0 is the desired linear gain, $z(n)$ is the input signal, $z_{pa}(n)$ is the output of the power amplifier, μ_g is the convergence constant for amplitude correction, μ_ϕ is the convergence constant for phase correction and k is the iteration index of the i^{th} LUT entry [9].

Mapping Predistorter:

Mapping predistorter was the first powerful digital predistorter based on a look-up table method, reported by Nagata [16]. Figure 2.19 shows the block diagram of the mapping predistorter. In mapping predistorter method, a two-dimensional LUT is used to map complex input signal to a new complex signal. The sum of the input signal and the LUT output approximates the inverse characteristics of the power amplifier. The amplifier output signal is synchronously demodulated and compared with the input signal [26]. The table entries are updated according to the results of this comparison.

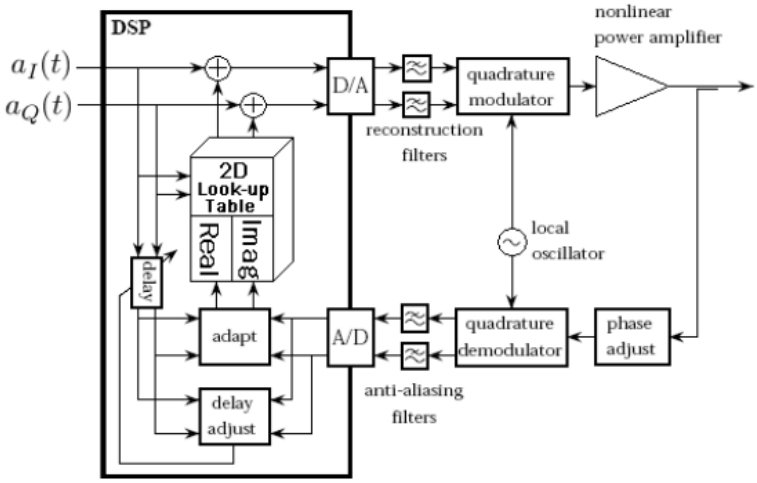

Figure 2.19: Mapping Predistorter
[25]

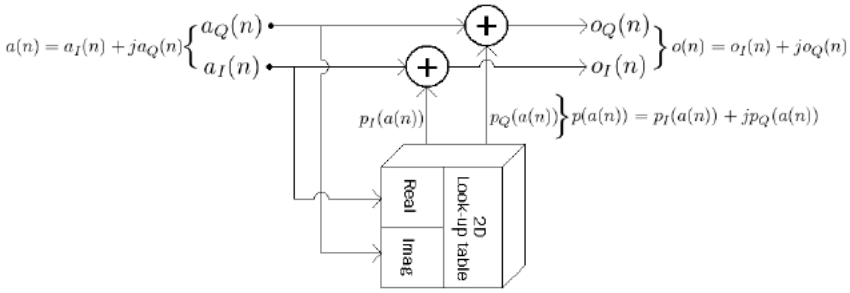

Figure 2.20: Mapping Procedure of Mapping Predistorter
[25]

Figure 2.20 shows the mapping operation of the predistorter. In the figure,

$a(n)$ is the predistorter input, $p(a(n))$ is the correction generated by the predistorter and $o(n)$ is the output signal.

$a(n) = a_I(n) + ja_Q(n)$;

$p(a(n)) = p_I(a(n)) + jp_Q(a(n))$;

$o(n) = a(n) + p(a(n)) = a(n) + p(a_I(n), a_Q(n))$;

$o_I(n) = a_I(n) + p_I(a_I(n), a_Q(n))$;

$o_Q(n) = a_Q(n) + p_Q(a_I(n), a_Q(n))$;

The above equations indicate that the I component and Q component correction values, p_I and p_Q, generated by the predistorter are functions of both the I and Q components of the input signal, a_I and a_Q, therefore the algorithm requires 2D LUT that are indexed by using both the I and Q components of the input signal. The adaptation algorithm of the mapping predistorter is as follows:

$$p_{ij}(k+1) = p_{ij}(k) + \mu(a(n) - \frac{a_{pa}(n)}{G}) \tag{2.15}$$

where $a(n)$ is the predistorter input signal and $a_{pa}(n)$ is amplifier output, signal$k$ is the number of iteration of the LUT cell which has index (i, j), μ is the convergence constant and G is the desired amplifier gain. The disadvantage of the mapping predistorter is its requirements of a large size LUT and its low adaptation speed.

Chapter 3

EFFECTS OF POWER AMPLIFIER NONLINEARITY AND MEMORY in COMMUNICATIONS SYSTEMS

This chapter describes the effects of power amplifier nonlinearity and memory. Common measures of power amplifier nonlinearity will be described in the first section. The second section will describe the common effects of power amplifier nonlinearity like harmonic distortion, spectral regrowth and intermodulation distortion. And finally the memory effects of power amplifiers will be presented.

3.1 Common Measures of Power Amplifier Nonlinearity

The two commonly used measures to describe nonlinearities of a power amplifier are 1dB compression point and third order intercept point [15]. In the following subsections, these two measures are described.

If a power amplifier is weakly nonlinear and has no memory, its input output relationship can be described by a polynomial with real coefficients:

$$y(t) = \sum_{n=1}^{\infty} c_n (x(t))^n = c_1 x(t) + c_2 (x(t))^2 + c_3 (x(t))^3 + ... \tag{3.1}$$

where c_1 is the linear small-signal gain of the amplifier, $x(t)$ is the input signal and $y(t)$ is the output signal. This polynomial model will be truncated to order 3 in the following subsections to find formulas for 1 dB compression point and 3^{rd} order intercept point.

3.1.1 1 dB Compression Point

1 dB compression point is defined as the power level where the gain of the amplifier deviates from the linear small signal gain by 1 dB. As the input power to an amplifier is increased, the amplifier enters its nonlinear region and the gain of the amplifier starts to decrease from its small signal value. The 1 dB compression point is reached when the compression in the gain reaches 1 dB. The 1 dB compression point (P_{1dB}) can be input power (IP_{1dB}) or output power (OP_{1dB}) referred and is usually given in units of dBm [15]. To measure the 1 dB compression point, a single tone signal $x(t) = Acos(w_0 t)$ is applied to the power amplifier and the amplitude A is increased from zero to higher values. If the nonlinear characteristic of the amplifier is given by 3.2 up to third order, the corresponding output signal will be :

$$y(t) = \frac{1}{2}c_2 A^2 + (c_1 A + \frac{3}{4}c_3 A^3)cos(w_0 t) + \frac{1}{2}c_2 A^2 cos(2w_0 t) + \frac{1}{4}c_3 A^3 cos(3w_0 t) \tag{3.2}$$

The gain at the fundamental frequency is given by $c_1 + \frac{3}{4}c_3A^2$. c_3 is negative and as a result, when the input amplitude A increases, the gain decreases. For small values of A, $c_1 \gg \frac{3}{4}c_3A^2$ and as a result, a linear gain of c_1 is obtained. As A increases, the gain compresses and when it compresses by 1 dB, the 1 dB compression point is reached. At the 1 dB compression point, $20log\left(\frac{c_1}{c_1+\frac{3}{4}c_3A^2}\right) = 1$ and the input amplitude at the 1 dB compression point is $A_{in1dB} = \sqrt{\frac{4}{3}\left|\frac{c_1}{c_3}\right|(1-10^{-\frac{1}{20}})}$. The following figure illustrates the 1 dB compression point graphically.

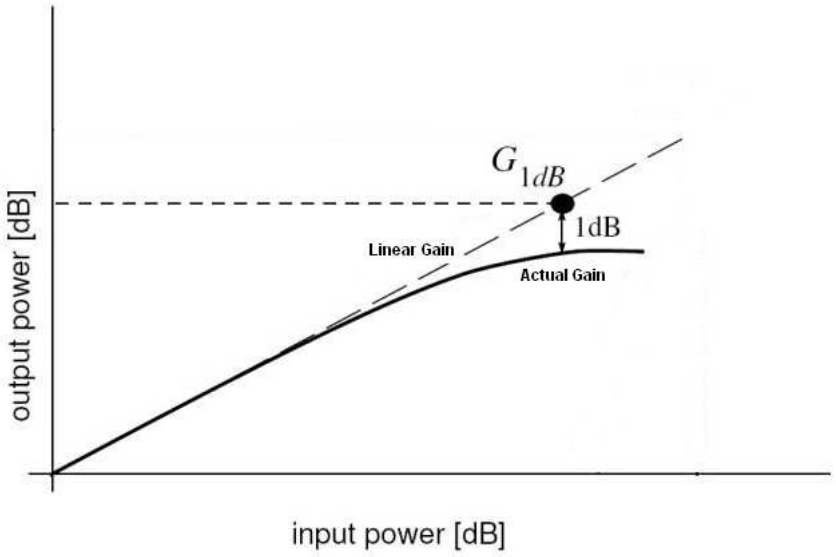

Figure 3.1: 1 dB Compression Point

3.1.2 Third order intercept point

If a two-tone signal $x(t) = Acos(w_1t) + Acos(w_2t)$ $(w_2 > w_1)$ is given as input to a nonlinear power amplifier, two main groups of distortion can be distinguished at the amplifier output. They are intermodulation products and harmonics [14]. The harmonics are produced at frequencies $nw1$ and $mw2$ $(n, m$ are integers) which are multiples of the fundamental frequencies w_1 and w_2. The harmonic products are typically out-of-band and they can be eliminated by filtering. The intermodulation products are produced at frequencies $\pm nw_1 \pm mw_2$. $|m| + |n|$

is called the order of the intermodulation products. Even-order intermodulation products are not so harmful because they are out-of-band and they can be eliminated by filtering. The odd-order intermodulation products are more harmful because many of them are in-band. Among the odd-order intermodulation products, the third order intermodulation products at frequencies $2w_1 - w_2$ and $2w_2 - w_1$ have the most important influence because they are the intermodulation products which are closest to the fundamental frequencies w_1 and w_2.

The third order intercept is defined as the point where third order intermodulation products (components at $2w_1 - w_2$ and $2w_2 - w_1$) at the amplifier output are equal in power to the fundamental components (w_1 and w_2) when the amplifier input is a two-tone signal. The third order intercept point is illustrated in the Figure 3.2.

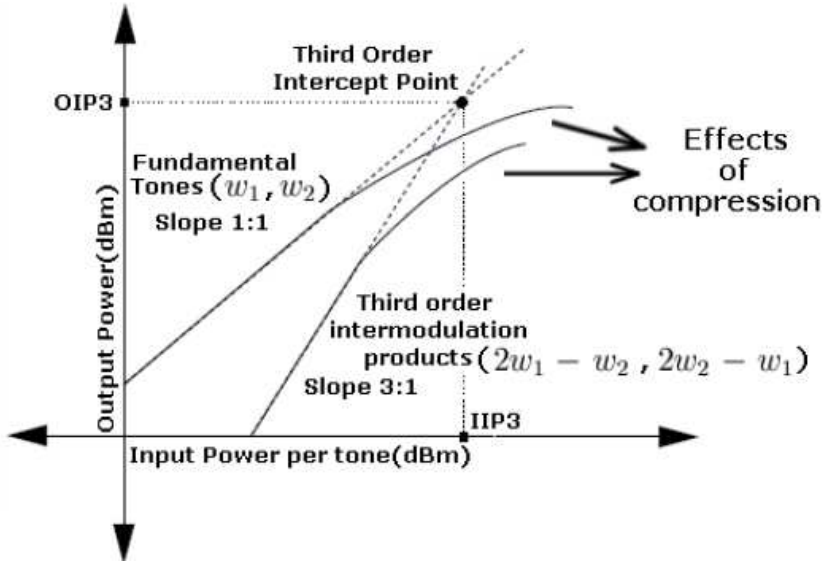

Figure 3.2: Third order intercept point

As seen in the figure, before compression both the power of fundamental tones and third order intermodulation products increase linearly with increasing power. For high input powers compression occurs. If the linear portions of both curves are extrapolated and intersected as seen in the figure, the third order intercept point is obtained.

If the input $x(t)$ is $x(t) = Acos(w_1 t) + Acos(w_2 t)$, then the corresponding

output $y(t) = c_1x(t)+c_2(x(t))^2+c_3(x(t))^3$ contains a lot of frequency components. The important ones are the frequency components at w_1, w_2, $2w_1 - w_2$ and $2w_2 - w_1$. The amplitude of the frequency components at w_1, w_2 is $c_1A + \frac{9}{4}c_3A^3$. The term $\frac{9}{4}c_3A^3$ causes compression for high input powers and it can be ignored in the calculation of the $IP3$ point. The amplitude of the frequency components at $2w_1 - w_2$, $2w_2 - w_1$ is $\frac{3}{4}c_3A^3$. At the third order intercept point, c_1A and $\frac{3}{4}c_3A^3$ should be equal to each other. Then the the input amplitude at the third order intercept point is found as:

$$A_{inIP3} = \sqrt{\frac{4}{3}\left|\frac{c_1}{c_3}\right|} \tag{3.3}$$

The third order intercept point can be input power or output power referred. If input power is used, it is called input third order intercept point and denoted by $IIP3$. If output power is used, it is called output third order intercept point and denoted by $OIP3$.

The 1 dB compression point and the third order intercept point are important parameters to characterize the nonlinearities of power amplifiers. They are generally provided by the amplifier manufacturers and they can be obtained by relatively simple measurements (single tone test $[input = Acos(w_0t)]$ and two tone test $[input = Acos(w_1t)+ = Acos(w_2t)]$) [14].

3.2 Effects of Power Amplifier Nonlinearity

In the following subsections, the nonlinear effects harmonic distortion, spectral regrowth and intermodulation distortion will be described.

3.2.1 Harmonic Distortion

When a single-tone signal at frequency w_0 is given as input to a nonlinear power amplifier, at the output of the amplifier we not only observe the excitation frequency w_0 but also the harmonic components at nw_0 (n integer) due to the nonlinearity of the power amplifier. This generation of harmonics of the excitation frequency by the nonlinear power amplifier is called harmonic distortion and the harmonic at frequency nw_0 is called n^th harmonic. THD (Total Harmonic Distortion) is a measure of Harmonic distortion which is defined as the ratio of the square roots of total harmonic output power to the output power at the fundamental signal.

3.2.2 Spectral Regrowth

The spectrum of the input signal to a power amplifier need not necessarily contain only discrete frequencies. If this input signal is a modulated signal that is commonly found in telecommunication systems, its spectrum will probably contain a continuous band of frequencies instead of discrete frequencies. When such a signal containing a continuous band of frequencies passes through a nonlinear power amplifier, this continuous band widens. This widening is called spectral regrowth. The figure 3.3 illustrates spectral regrowth of a signal caused by a nonlinear amplifier.

Due to spectral regrowth, leakage into adjacent bands (channels) occurs. This leakage causes interference for the adjacent channel and is called adjacent channel interference. Figure 3.4 illustrates adjacent channel interference. An important measure of adjacent channel interference is $ACPR$ (Adjacent Channel Power Ratio). $ACPR$ can be defined as total adjacent channel power ratio ($ACPRT$), which is the ratio of total output power measured in the main channel to the total power integrated in the lower and upper adjacent channel bands.

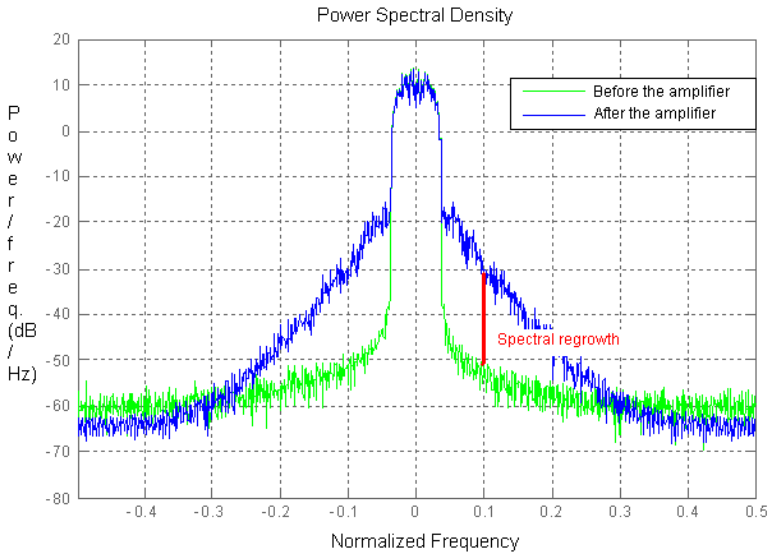

Figure 3.3: Spectral Regrowth

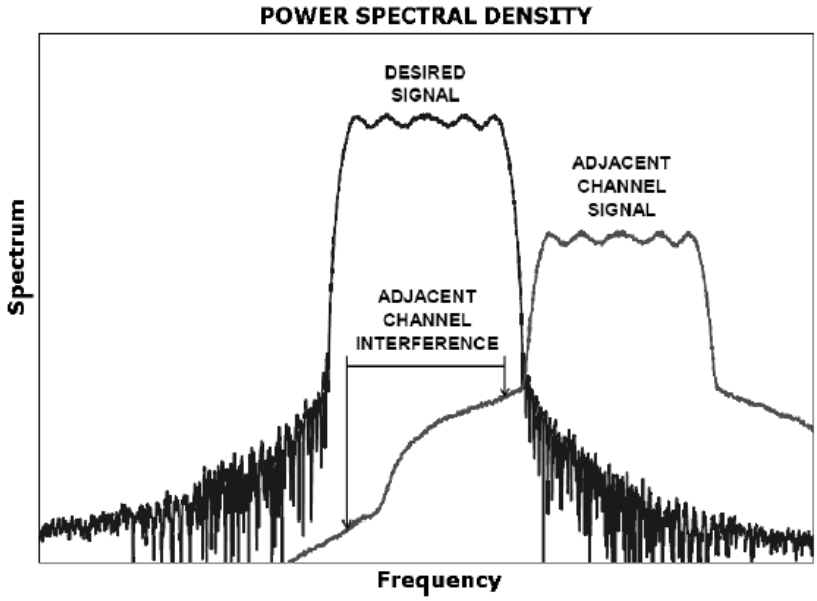

Figure 3.4: Adjacent Channel Interference

3.2.3 Intermodulation Distortion

When a multi-tone signal (containing more than one fundamental frequency) is given as input to a nonlinear power amplifier, at the output of the amplifier we only only observe the excitation frequencies and their harmonics but also the linear combinations of the excitation frequencies. For instance if the input is a two-tone signal ($cosw_1$; $cosw_2$), at the output we will observe the harmonics nw_1 and mw_2 and also the components at the frequencies $\pm mw_2 \pm nw_1$. These linear combinations of the excitation frequencies are called intermodulation products and this type of distortion is called intermodulation distortion. $k = |m| + |n|$ is the order of the intermodulation distortion and the corresponding intermodulation products at frequencies $\pm mw_2 \pm nw_1$ are called the k^th order intermodulation products. An important measure of intermodulation distortion is IMR (intermodulation ratio) which is defined as the ratio of the fundamental output power to the intermodulation distortion output power.

3.3 Memory Effects in Power amplifiers and the Modeling of the Memory Effect

3.3.1 Memory Effects in Power Amplifiers

Memory effects are defined as changes in the amplitude and phase of distortion components caused by changes in modulation frequency. Mechanisms with different time-constants, mainly related to the biasing system and heat-generation cause spectral regrowth and sideband asymmetries. This can be observed both for analog signals as IMD asymmetry and for digitally modulated signals as regrowth asymmetry (Figure 3.5).

Much work on memory-effects is related to behavioral modeling of power amplifiers. These models will be described in the following sections. Sources of memory effects can be classified as electrical and thermal. We will basically

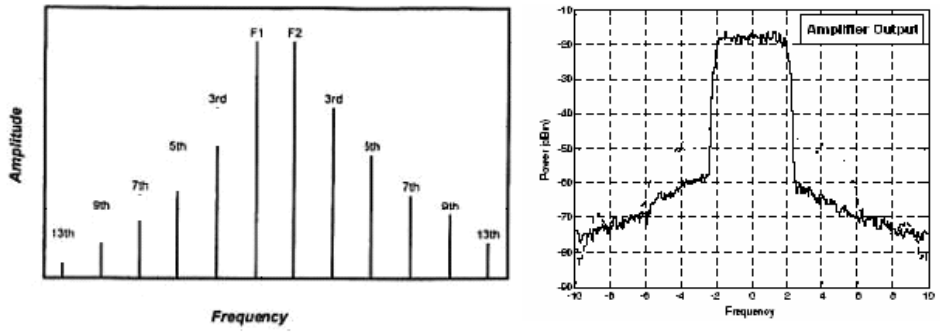

Figure 3.5: IMD Asymmetry and Regrowth Asymmetry Effects of Memory

consider electrical memory effects.

As stated in section 3.1.2 the the amplitude for both the lower and upper third order intermodulation (IM3) sidebands can be written as $\frac{3}{4}c_3A^3$ for the input $x(t) = Acos(w_1t) + Acos(w_2t)$, and the corresponding output $y(t) = c_1x(t) + c_2(x(t))^2 + c_3(x(t))^3$. It is seen from these equations that the amplitude of IM3 sidebands increases exactly to the third power of the input amplitude. Unfortunately, the power amplifiers with memory do not behave like this. For example, the envelope signal ($w_2 \;\; w_1$) and the upper two-tone signal (w_2) will be mixed with the second-order nonlinearity, which results in the generation of an IM3 signal in addition to the IM3 component with the amplitude of $\frac{3}{4}c_3A^3$. Similarly, the second harmonic of the upper input signal ($2w_2$) and the lower input signal from the negative frequency side ($-w_1$) will produce an IM3 signal. As a result, IM3 sidebands are affected not only by fundamental voltage waveforms, but also by the voltage waveforms at the frequency of the envelope ($w_2 - w_1$). In addition, the second harmonics ($2w_1$ and $2w_2$) also affect the IM3 sidebands. The greatest part of the distortion is produced by third-order distortion mechanisms, which are affected by fundamental impedance. However, second-order mechanisms generated by the envelope and second harmonic frequencies also have a significant effect on IM3 distortion and causes asymmetries in IM3 components and spectral regrowth. Since the linearities of the circuit components can be considered as current sources, their voltage waveforms can be affected by node impedances [27]. Node impedances consist of two parts: internal impedance of the amplifier and external impedance. External impedance also comprises two

parts: the impedance of the matching network and that of the bias network. The combined effects of these impedances must be considered in the design of well-behaving node impedances. It is mentioned in literature that the major part of the memory is produced by envelope impedances. Envelope frequency varies from dc to the maximum modulation frequency, which can be as high as a few megahertz. Therefore, minimizing memory effect is a critical issue in the design of the power amplifier. The output impedance, for example, must be constant or very low over this region in order to avoid memory effects. The reason of considering memory effect in this thesis is that that memory effects is a serious limitation on the maximum achievable cancellation performance of the linearization method.

3.3.2 Modeling of the Memory Effect

A nonlinear power amplifier with memory can be represented by Volterra series or linear time-invariant (LTI) system followed by a memoryless nonlinearity known as Hammerstein model or Nonlinear tapped delay line (NTDL).

3.3.2.1 Volterra Memory Model

A truncated discrete time domain Volterra model for power amplifier has the form :

$$\mathrm{y(n)} = \mathrm{h}_0 + \sum_{k_i=0}^{m-1} h_i(k_i)x(n-k_i)$$

$$+\sum_{k_i=0}^{m-1}\sum_{k_2=0}^{m-1} h_2(k_i,k_2)x(n-k_i)x(n-k_2) + ...$$

$$+\sum_{k_i=0}^{m-1}.....\sum_{k_p=0}^{m-1} h_p(k_i,.....,k_p)x(n-k_i).....x(n-k_p)$$

where h_0 is a constant and $h_j(k_i,.....k_j)$ are the set of j^th order Volterra Kernel coefficients [18].

Literature shows that implementing Volterra predistorter is computationally intensive and in addition, an accurate inverse of Volterra system is difficult to obtain and the jth order inverse is only an approximation.

Zhus [28] simulation for third order Volterra based linearizer shows about 10 dB improvements in the IMD performance of the power amplifier with the signal bandwidth of approximately 4 MHz. The reason for only a 10 dB improvement may be attributed to the fact that an exact inverse for Volterra model is difficult to attain.

3.3.2.2 Hammerstein Memory Model

Hammerstein predistorter model is represented by the equation:

$$z(n) = \sum_{p=1}^{P} a_p z(n-p) + \sum_{q=0}^{Q} b_q \left(\sum_{k=0}^{\frac{(k-1)}{2}} c_{2k+1} y(n-p) \left| y(n-q) \right|^{2k} \right) \tag{3.4}$$

where the $y(n)$ is the input and $z(n)$ is the output and the algorithm computes the a_p, $b_q$and c_{2k+1} coefficients.

A hammerstein predistorter model example can be found in [7]. The adaptive Hammerstein predistorter in [7] uses an indirect learning architecture and consists of predistorter trainer and a predistorter, the LTI portion is implemented using a FIR filter. An iterative estimation algorithm in the predistorter trainer computes the inverse model of power amplifier and copies the coefficients in the predistorter in the forward path until loop converges. [7] states over 35 dB of improvement in the IMD performance of the power amplifier.

3.3.2.3 Nonlinear Tapped Delay Line Memory Model

The memory is characterized in the power amplifier as hysteresis in AM/AM and AM/PM curves and can be represented by a tapped delay line polynomial as shown in figure 3.6. The hysteresis in the power amplifier is represented by complex gain polynomial at each tap. The polynomial at each tap is of odd order to ensure the amplifier is compressed by the same amount for both positive and negative voltages. The amplifier with memory can be represented by:

$$y(k) = \sum_{m=0}^{m=M} z_{k-m} \sum_{j=0}^{p} A_j \, |z_{k-m}|^{j-1} \tag{3.5}$$

The p is the order of the polynomial and A_js are complex coefficients.

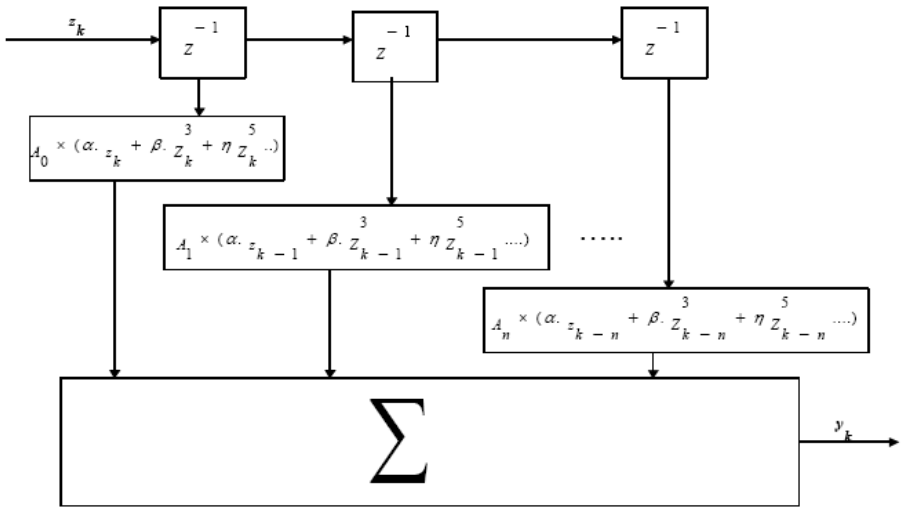

Figure 3.6: NTDL Power Amplifier Model

An adaptive NTDL predistorter uses an indirect learning architecture as shown in Figure 3.6 and consists of a trainer NTDL and a predistorter NTDL [17]. Each tap in the NTDL predistorter is a look-up table. A polynomial fit is performed by the trainer. The trainer first estimates inverse nonlinear parameters of the power amplifier and calculates the coefficients for the polynomial in the NTDL. The trainer then fits the polynomial in the look-up table for each tap in the predistorter. In [17], the simulation results show that for 3-tap 6th order polynomial, the IMD performance is improved by 30 dB for a 2-carrier WCDMA which has a signal bandwidth of 10MHz.

Chapter 4

IMPLEMENTATION of a COMPLEX GAIN BASED LOOK-UP TABLE PREDISTORTER in software

This chapter describes the implementation of complex gain based predistorter in Matlab and Simulink. In the implementation Communications Blockset, Signal Processing Blockset and Memoryless Nonlinearity Blockset are used.

The proposed model is a baseband system model. Each element of the system will be described in detail in the following sections. After the description of the system elements, the simulation results will be presented.

4.1 Complex Gain-Based Predistorter Matlab Model

The simulated baseband communication transmitter model is shown in Figure 4.1. Each of the element in the model is represented by its baseband equivalent.

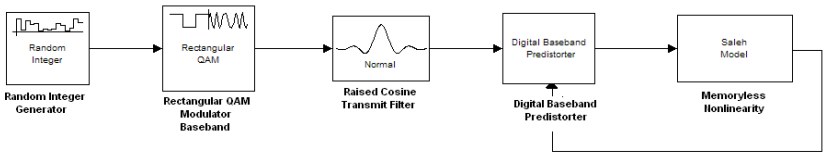

Figure 4.1: Simulated System Model

4.1.1 Random Integer Generator

The Random Integer generator block generates uniformly distributed random integers in the range $[0, M-1]$, where M is used as 16 in the simulations. Since M is chosen as a scalar, then all output random variables are independent and identically distributed (i.i.d). The output signal can be a frame-based matrix or a sample-based row or column vector. Since the system is a sample-based model, the output of the Random Integer Generator is chosen as a sample-based one dimensional array.

4.1.2 Rectangular QAM Modulator

QAM stands for quadrature amplitude modulation which conveys data by changing (modulating) the amplitude of two carrier waves. These two waves, usually sinusoids, are out of phase with each other by 90 and are thus called quadrature carriers. These two carriers are called I and Q channels. The carrier of I (in phase) channel is a cosine wave while the carrier of Q (quadrature) channel is a sine wave. So by amplitude modulating I and Q channels, quadrature amplitude modulation is obtained. The type of the QAM modulation depends on the number of points in their constellation. If the constellation contains M points, it is called M-QAM modulation. All the constellation points of M-QAM modulation are complex numbers. The real parts of the constellation points represent the I channel modulation and the imaginary parts of the constellation points represent the Q channel modulation. The modulator used in the simulink model is $16-QAM$ modulator. In the constellation, a Gray coded bit-assignment is also given so that adjacent elements differ only by one bit. After the modulation of the input signal it is necessary to apply upsampling and pulse- shaping filtering in

order to limit the bandwidth of the transmitted signal. Both of the requirements are satisfied by using a Raised Cosine Transmit Filter.

4.1.3 Raised Cosine Transmit Filter

In telecommunication, intersymbol interference (ISI) is a form of distortion of a signal in which one symbol interferes with subsequent symbols. Raised cosine filters are widely used to eliminate ISI. The raised-cosine filter is an implementation of a low-pass Nyquist filter, one that has the property of vestigial symmetry. This means that its spectrum exhibits odd symmetry about $\frac{1}{2T}$, where T is the symbol-period of the communications system. Its impulse response description is given by:

$$h(t) = \frac{sin(\pi \frac{t}{T})}{\frac{\pi t}{T}} * \frac{cos(\frac{\pi R t}{T})}{1 - \frac{4R^2t^2}{T^2}} \tag{4.1}$$

As seen in the Equation 4.1 the raised cosine filter is characterized by two values; R, the roll-off factor, and T, the reciprocal of the symbol-rate. The roll-off factor, R, is a measure of the excess bandwidth of the filter, i.e. the bandwidth occupied beyond the Nyquist bandwidth of $\frac{1}{2T}$. If we denote the excess bandwidth as Δf, then: $R = 2T\Delta f$.

The AM/AM parameters, α_a and β_a are used to compute the amplitude gain for an input signal. The Figure 4.2 shows the amplitude response as R is varied between 0 and 1, and the corresponding effect on the impulse response. As can be seen, the time-domain ripple level increases as R decreases. This shows that the excess bandwidth of the filter can be reduced, but only at the expense of an elongated impulse response. Raised cosine filter blockset used in the simulation also allow applying upsampling. By setting upsampling factor N, $N - 1$ zeros are inserted between consecutive complex information signals coming from the $16 - QAM$ modulator. By upsampling sampling frequency increases by a factor of N. The increment of the sampling frequency also increases the observable spectral range that we need in order to observe out-of-band spectral components.

In the proposed simulation model N is equal to 24 and R is equal to 0.2.

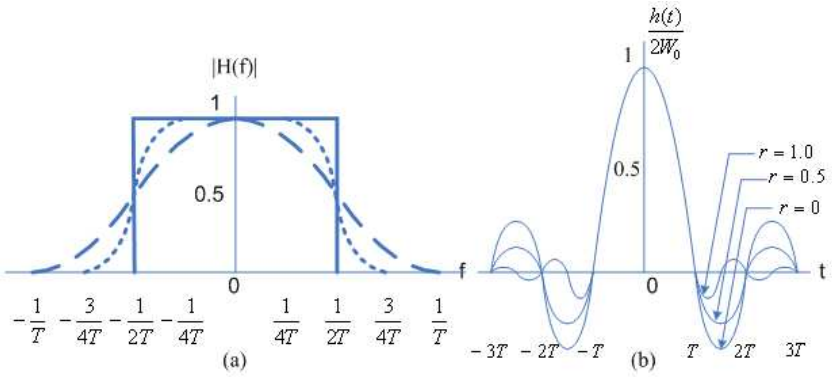

Figure 4.2: Raised Cosine Filter Response with varying R

4.1.4 Saleh Model Memoryless Nonlinearity

For an ideal linear amplifier there is a linear relationship between input power output power. But unfortunately, this is not the case in real systems. Figure 2.1 shows that as the input amplitude increases, the linear behaviour of the amplifier is disturbed, amplifier gain compresses and starts to decrease. As the input power increases, the output power takes values smaller than the ideal linearly amplified value. This behaviour of the amplifier is called AM/AM characteristics of the amplifier. Additionally, ideal linear amplifier inserts a zero phase shift or a constant phase shift to the input signal at all its power levels. Once again unfortunately, this is not the case in real systems. As the input power increases, the phase shift applied to the input signal by the amplifier changes. This behaviour of the amplifier is called AM/PM characteristics of the amplifier.

The AM/AM and AM/PM responses of a power amplifier can be measured by applying a single tone input signal to the amplifier and sweeping the power of this input signal. A model can then be fitted to the measured data [14]. There are several models in the literature used for modeling power amplifier AM/AM and AM/PM responses. These are Saleh model, Rapp model, third order polynomial model and arctan model. In this thesis the proposed memoryless nonlinearity

model is the *Saleh Model*. Saleh model uses the following equations to model AM/AM and AM/PM responses of a power amplifier:

$$F_{AM/AM}(u) = \frac{\alpha_a * u}{1 + \beta_a * u^2} \tag{4.2}$$

$$F_{AM/PM}(u) = \frac{\alpha_p * u^2}{1 + \beta_p * u^2} \tag{4.3}$$

The AM/AM parameters, α_a and β_a are used to compute the amplitude gain for an input signal. The AM/PM parameters, α_p and β_p are used to compute the phase change for an input signal. U represents the magnitude of the scaled signal. The following Figure 4.3 is an example of AM/AM conversion and AM/PM conversion of the Saleh model nonlinearity.

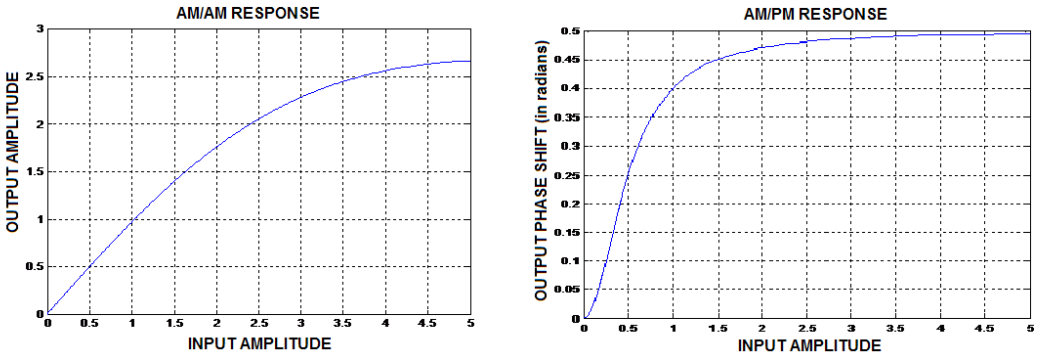

Figure 4.3: AM/AM and AM/PM characteristics of a Saleh Model

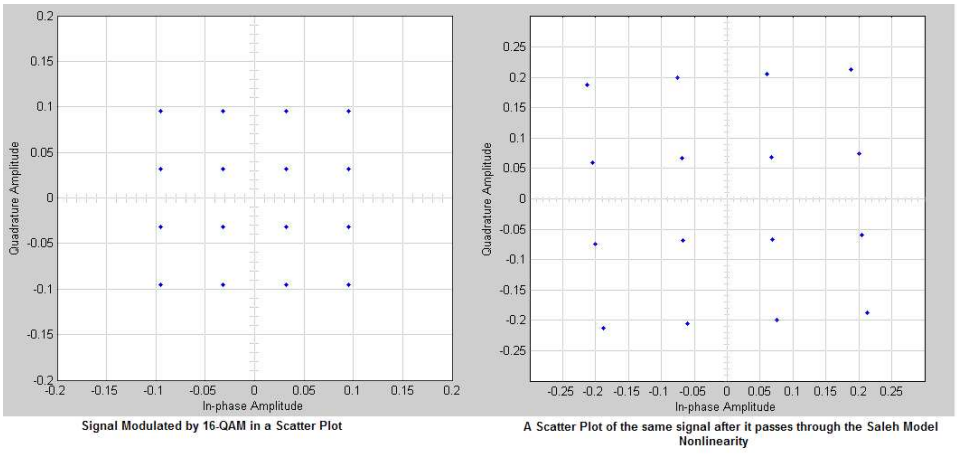

Figure 4.4: The Nonlinearity Generated by Saleh Model

In Figure 4.4, it is possible to see the effect of the memoryless nonlinearity block on a signal modulated by $16-QAM$. It is easy to observe from the figure that both the amplitude gain and the phase shift are not constant for all input amplitude levels.

4.1.5 Adaptive Digital Baseband Predistorter

As indicated in Chapter 2, this thesis proposes a method of LUT predistortion using direct predistorter adaptation. The following section will describe the proposed predistortion method in detail in terms of predistorter table, table addressing, table adaptation and delay adjustment estimation.

4.1.5.1 Predistorter Table and Table Addressing

In the literature, it is observed that almost in all methods the LUT is addressed by the magnitude of the source signal so the error is distributed throughout the table, so more accurate predistortion output is obtained at all power levels. However, since magnitude squared is easier to calculate, this may also be used to address the table. The magnitude squared addressing is called power addressing in the literature. The power addressing concentrates the entries to high amplitudes thus making low amplitude coarse. This is acceptable since majority of distortion is caused when the amplifier is operated close to the compression region. The sensitivity of the algorithm to both magnitude addressing and power addressing will be presented in Chapter 5. The Figure 4.5 shows the address calculation of the LUT. Either the magnitude or the magnitude square of the input is calculated and the result is used to address the complex gain LUT.

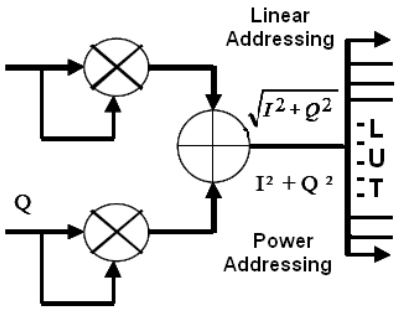

Figure 4.5: Look-up Table Address Calculation

4.1.5.2 Look-up Table Adaptation

There are various techniques described in the literature for adaptation of look-up table entries, such as linear convergence, secant method and rotate and scale method. The method of adaptation selected will determine speed of convergence, stability of the system, and computation load.

The linear convergence is based on classical feedback theory, and it is computationally simplest and the least stable for adaptation look-up table entries. The error ($V_{err}(t) = V_{mod}(t) - V_{fb}(t)$) in linear convergence is modified by the adaptation constant "a" and resulting $V_e(t)$ is summed with the previous entry in the table $F_i(k)[Re(V_e), Im(V_e)]$. The new entry in the table is $F_i(k+1)[Re(V_e), Im(V_e)]$ and is stored at the magnitude envelope address of $V_{mod}(t)$ (see Figure 4.6). This iteration update occurs every time the modulating signal envelope passes through a given table entry. The subscript "i" represents a specific entry in the table and k represents the k_{th} iteration. The adaptation constant "a" is generally selected to be less than unity and controls the rate of convergence [19].

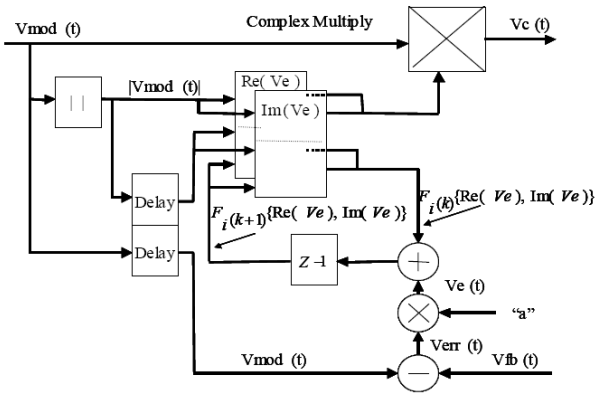

Figure 4.6: Linear Convergence Model
[19]

The secant adaptation method is based on a straight line approximation. The function $f(x)$ is being approximated by a straight line which is an extrapolation based on the two points x_i and x_{i-1}. Using some geometry the Equation 4.4 is obtained.

$$\frac{f(x_i)}{x_i - x_{i+1}} = \frac{f(x_{i-1})}{x_{i-1} - xi + 1}; \tag{4.4}$$

Applying the secant method of convergence for adaptation of look-up table entries is given by the following equation,

$$F_i(k+1) = \frac{F_i(k-1)e_g(F(k)) - F_i(k)e_g(F(k-1))}{e_g(F(k)) - e_g(F_i(k-1))}; \tag{4.5}$$

where $F_i(k)$ is the k_{th} iteration of look-up table entry i and e_g is the quantization error at the PA output. For detailed derivation of Equation 4.5 refer to [3].

The rotate and scale method of adaptation is used for polar tables and is similar to the linear convergence method described above. Rearrangement of equation ($V_{err}(t) = V_{mod}(t) - V_{fb}(t)$) gives:

$$|V_{err}(t)| = |V_{mod}(t)| - |V_{fb}(t)|; \tag{4.6}$$

$$\angle V_{err}(t) = \angle V_{mod}(t) - \angle V_{fb}(t); \tag{4.7}$$

The gain and phase look-up table entry update at k_{th} iteration is given by:

$$F_i(k+1)(|V_e|) = F_i(k)(|V_e|) + a|V_{err}|; \tag{4.8}$$

$$F_i(k+1)(\angle V_e) = F_i(k)(\angle V_e) + a\angle V_{err}; \tag{4.9}$$

Cavers states in [3] that the linear convergence method reported by Nagata [16] is the best so far of the linear convergence methods. In favor of this adaptation algorithm is the low computational load: each iteration requires three complex additions, a real by complex multiplication and no divisions. On the other hand, the number of iteration required is very high compared to the secant method [3]. Cavers also states that each table entry needs about ten iterations for convergence in the secant method of adaptation. The drawback of the secant method is its computational load. From equation 4.5, each iteration requires two complex additions, four complex multiplications, and two complex by real divisions.

The proposed table adaptation method is similar but different than the ones in the literature. It is first proposed by Burak Şekerlisoy [23].

The Figure 4.7 shows the overall matlab model.

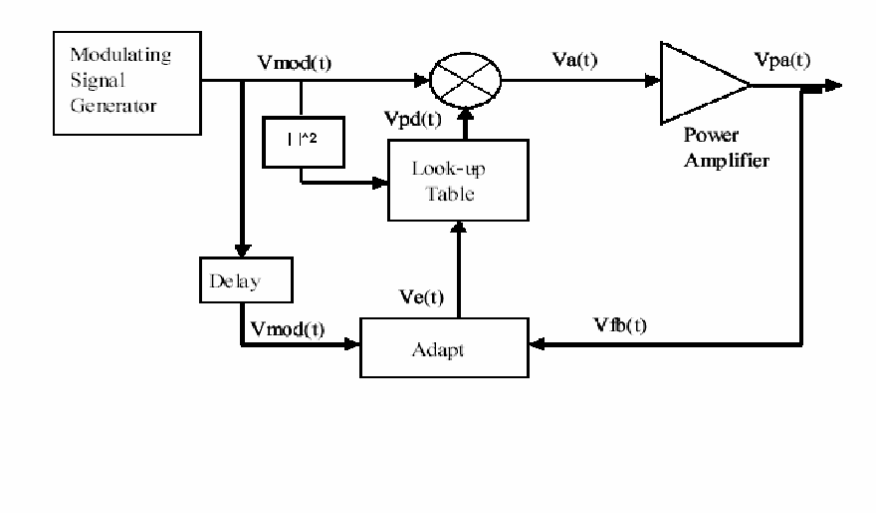

Figure 4.7: Complex Gain-Based Predistorter Matlab Model

The complex envelope of the input V_a and the output V_{pa} of the power amplifier are related by:

$$V_{pa} = V_a(t) * G[|V_a(t)|^2]; \tag{4.10}$$

where $G[|V_a(t)|^2]$ is the complex gain of the amplifier. The gain function from the look-up table is multiplied with modulated input signal.

$$V_a(t) = V_{mod}(t) * F[|V_{mod}(t)|^2]; \tag{4.11}$$

where $F[|V_{mod}(t)|^2]$ is the complex gain of the predistorter stored in the LUT . For the adaptation of look-up table the following Equation 4.12 is used. Then, The updated table entry is:

$$F_i(k+1) = F_i(k) + \alpha(V_{fb}(t) - V_{mod}(t))(-conj(V_{mod}(t)); \tag{4.12}$$

Where $F_i(k)$ is the i_{th} table entry in k_{th} iteration and α is the adaptation constant. The proposed algorithm requires complex multiplications and additions, but no divisions. This decreases the computational load.

4.1.5.3 Delay Adjustment Estimation

The propagation delays in transmit and receive path results (see Figure 4.8) in the sampled feedback signal $V_{fb}(n)$ being of later time interval then the input complex signal $V_{mod}(n)$. This delay has to be accurately computed so the time aligned $V_{fb}(n)$ and $V_{mod}(n)$ can be compared to generate the error vector $V_e(n)$. If the delay is not computed accurately, then the adaptation tables will have noise distortion component in the tables resulting in a less accurate inverse table. Therefore, the distortion products generated by the power amplifier will not be cancelled resulting in a non optimal predistortion correction. A simple method for compensation of delay in feedback sample $V_{fb}(n)$ is to delay the input sample $V_{mod}(n)$ by the required number of samples before a comparison is made between the input and the feedback samples.

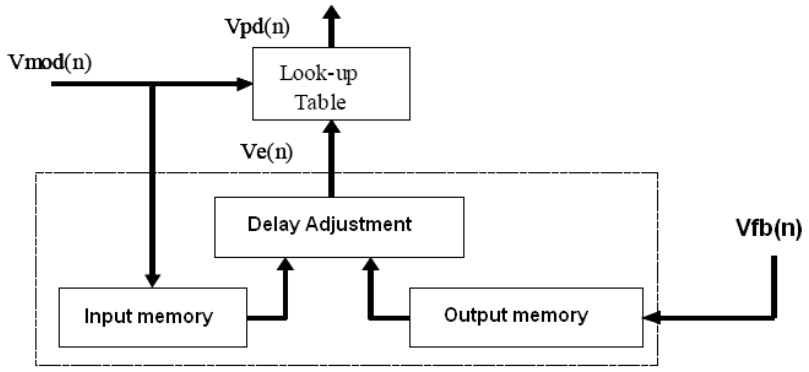

Figure 4.8: Delay Adjustment Estimation

There are several techniques described in the literature to compute the delay which exits in the forward and the feedback paths of the PA chain. A common technique to determine the delay requires the use of cross correlation between the input $V_{mod}(n)$ and the feedback $V_{fb}(n)$ samples to determine the delay. This method requires a block of input and feedback samples to be stored. The cross correlation of the two series is calculated. The cross correlation of V_{mod} and $V_{fb}(n)$ in discrete time domain is defined as:

$$R_{V_{mod}V_{fb}}[n] = \frac{1}{N}\sum_{k=n}^{n+N-1} V_{mod}[k-n]V_{fb}[k] = \frac{1}{N}\sum_{m=0}^{N-1} V_{mod}[m]V_{fb}[m+n], m \geq 0; \tag{4.13}$$

The sum will be maximum when the two samples' streams line up. Therefore, delay between the two signals is from origin to time where the peak occurs in their cross correlation as shown in Figure 4.9.

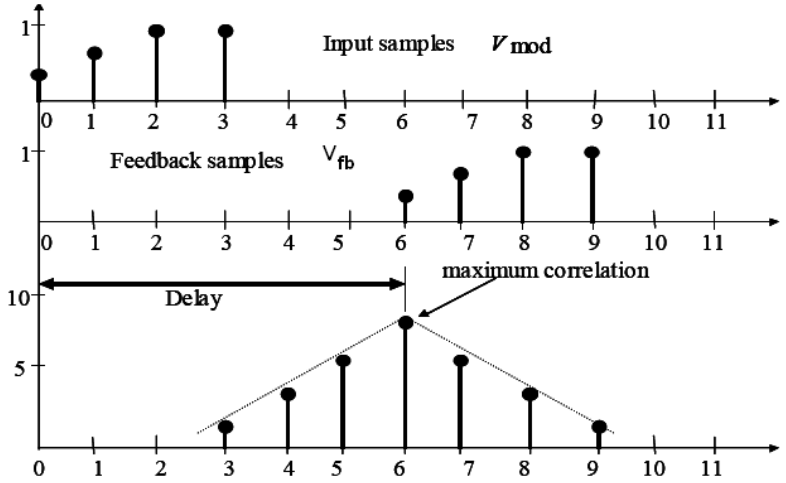

Figure 4.9: Cross Correlation Block Diagram

Other techniques employed for delay estimation are by comparing the slope of the magnitude of the input and feedback to determine direction of delay adjustment. The amount of delay d_i at time t_i can be examined by the following relation between a signal $q(t)$ and its delayed version q(t-r).

$d_i = d_{i-1} + sgn[(q(t_i) - q(t_i - d_{i-1}))]$ if $q'(t_i)$ >Threshold

$d_i = d_{i-1} - sgn[(q(t_i) - q(t_i - d_{i-1}))]$ if $q'(t_i)$ <-Threshold

The details of the above method can be found in [16]. This method of delay estimation is also applied to the proposed predistortion method. Because the high number of iteration requirement of the method, it is decided to use cross correlation method for the rest of the implementation.

In this chapter the model used and the methods of the table addressing, table adaptation and delay adjustment are explained. The following chapter will demonstrate the simulation results and response analysis of the predistorter.

Chapter 5

RESPONSE ANALYSIS of the proposed PREDISTORTER

Response analysis of the predistorter is performed to determine which parameters of the adaptive digital predistortion system improves or degrades the distortion correction performance. The distortion improvement in power spectrum is accepted as the main criterion. The predistorter response to adaptation constant, table addressing, table size, input-output delay alignment, memory effect and the number of iteration are examined. The results will be presented in the following sections.

5.1 Response of the Predistorter to Adaptation Constant(α)

As mentioned in Chapter 4, the LUT adaptation algorithm is $F_i(k+1) = F_i(k) + \alpha(V_{fb}(t) - V_{mod}(t))(-conj(V_{mod}(t))$, where α is called the adaptation constant. The adaptation constant α is generally selected to be less than unity ($0 < \alpha < 1$). The adaptation constant controls the rate of convergence. If the α is large then there exists a possibility that the table entries will not converge, but oscillate

and result in an unstable system. If the adaptation constant α is small then the adaptation time gets longer and with less number of iteration we may get worse distortion improvement. The Figure 5.1 shows the algorithm response to constant α.

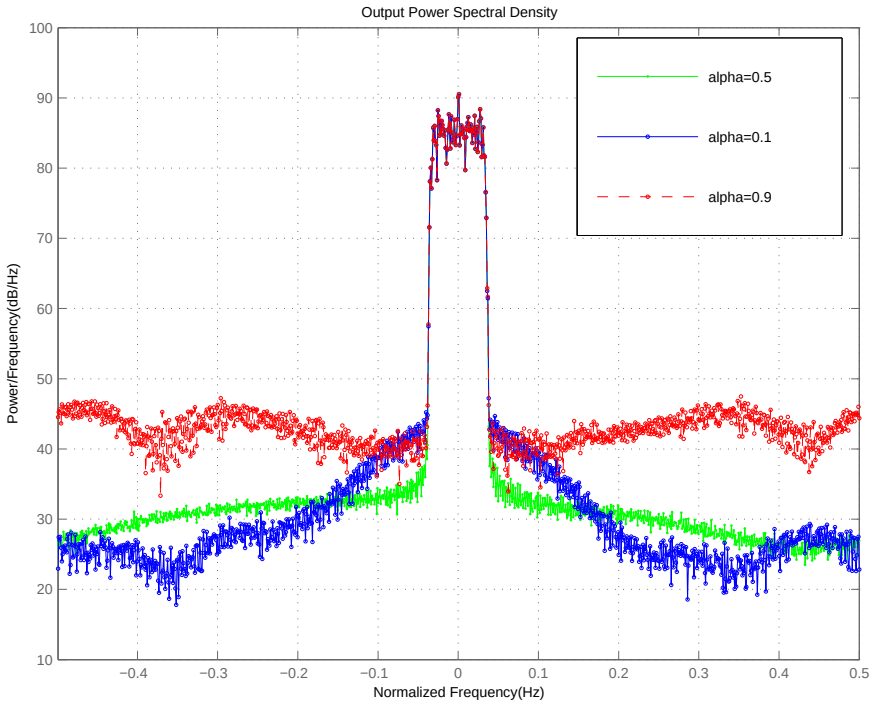

Figure 5.1: Sensitivity to Adaptation Constant

It is observed that the optimum value for the adaptation constant is around 0.5. The optimal value of α leads to an approximately 10 dB of additional improvement in the performance of the predistorter as compared to $\alpha = 0.1$ and $\alpha = 0.9$ cases. For all other response analysis the adaptation constant α is chosen as 0.5.

5.2 Response of the Predistorter to the Table Addressing

In Chapter 4 the two addressing methods (power addressing and linear addressing) are presented. The look-up table is addressed by linear method addressing

where the magnitude of the source signal is used and power method of addressing where the magnitude square of the source signal is used. The figure 5.2 shows the algorithm response to these two different table addressing methods.

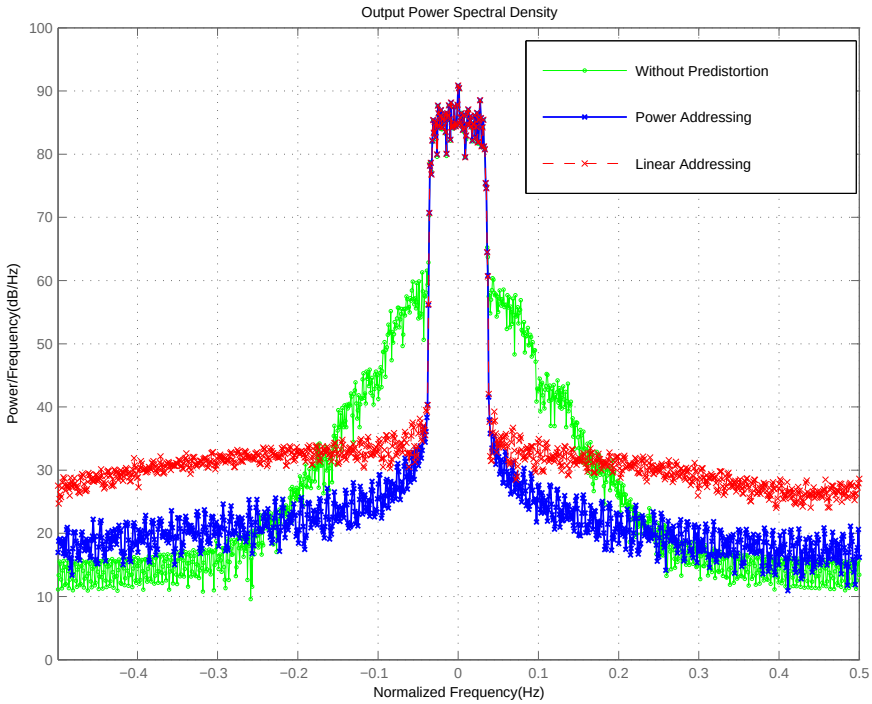

Figure 5.2: Sensitivity to Table Addressing

Since the majority of distortion is caused when the amplifier is operated close to the compression region. Then the power method of addressing concentrates high amplitude table entries thus making low amplitude coarse. Figure 5.2 shows that power method of addressing leads to an approximately 6 dB of additional improvement in the performance of the predistorter.

5.3 Response of the Predistorter to Table Size

The number of entries of the LUT is called table size and it is an important parameter in terms of predistorter gain component convergence and adaptation time. The adaptation table size is adjusted in steps of 32 entries, 128 entries and 256 entries. Figure 5.3 shows the improvement in the spectral response with a

digital predistorter using a look-up-table size of 32. Notice that the background noise level is increased compared to the original waveform. The background noise originates from discontinuities in the predistortion function. It is expected that increasing the table size will reduce the size of discontinuities and hence the background level.

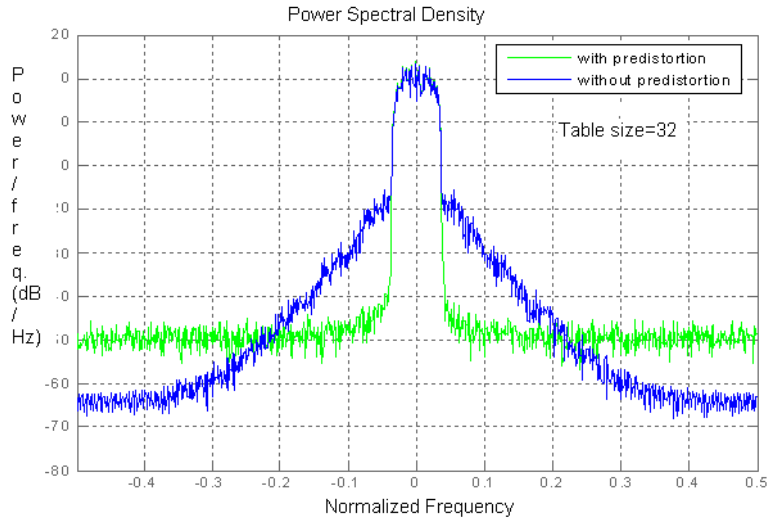

Figure 5.3: Simulated output spectrum with and without predistortion for the QAM input signal for a LUT size of 32.

We note that long sequences of input data need to be used to achieve convergence of the algorithm. This involves Matlab runs of couple of hours on a modern computer.

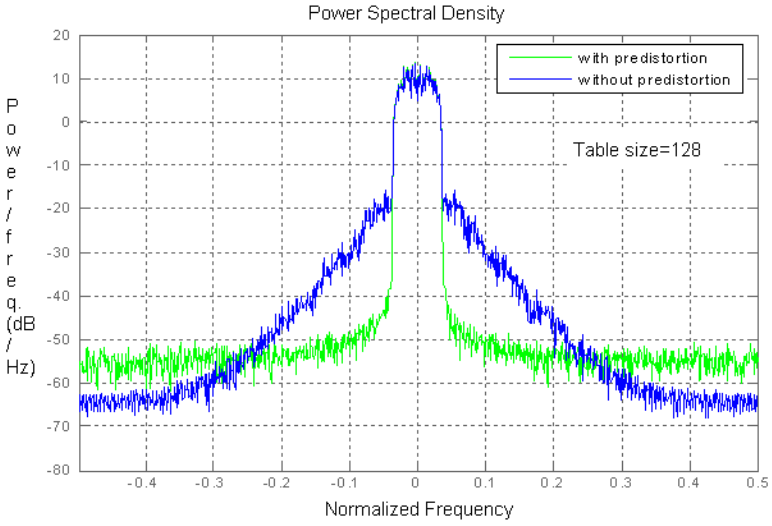

Figure 5.4: Simulated output spectrum with and without predistortion for the QAM input signal for a LUT size of 128.

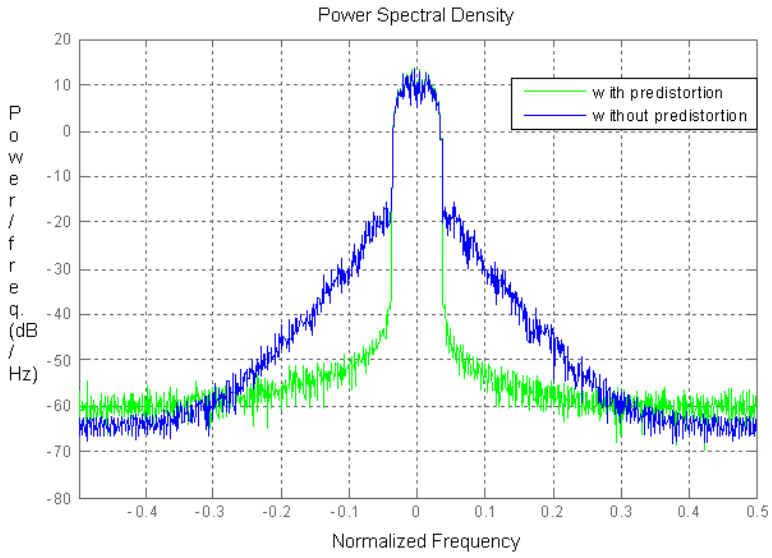

Figure 5.5: Simulated output spectrum with and without predistortion for the QAM input signal for a LUT size of 256.

Figure 5.4 shows simulation results for a look-up-table size of 128. Indeed, the background noise level in this case is improved by about 5 dB. Figure 5.5 is for similar results for a table size of 256. The background level here is another 5 dB below. For small table sizes, the input amplitude range addressed to the same entry increases and this situation causes discontinuities and background noise.

It is shown with Matlab simulations that it is possible to obtain up to 25 dB improvement in power spectrum and sufficiently large look-up-table needs to used to reduce the background noise level and the discontinuities in the predistortion function.

5.4 Response of the Predistorter to Delay Alignment

The simulation model is a sample-based system. There is integer number of delays between the input signal from the tone generator and the feedback from the PA. Chapter 4 explains that cross correlation between the input $V_{mod}(n)$ and the feedback $V_{fb}(n)$ is used to determine the delay. In a real system delay will not be an integer multiple of sample period. Let's say that the real delay component is the addition an integer multiple of and a fractional multiple of sample period. Since the cross correlation method manages to find the integer multiple part of the delay, misalignment by half sample is accepted as the worst case for the fractional multiple part. The impact on power spectrum if the input and feedback are misaligned by half sample is shown in Figure 5.6. The comparison between Figure 5.6 and no fractional delay case shown in Figure 5.7 indicates that misalignment by half sample degrades the distortion improvement performance by approximately 15 dB.

We have also observed that in order to maintain sufficient linearity improvement the alignment should be within $\frac{1}{80}$ of sample period. It is shown in Figure 5.8, if the alignment is within $\frac{1}{80}$ of sample period 25 dB distortion improvement can be achieved, otherwise the improvement decreases to 10 dB. Nagata states

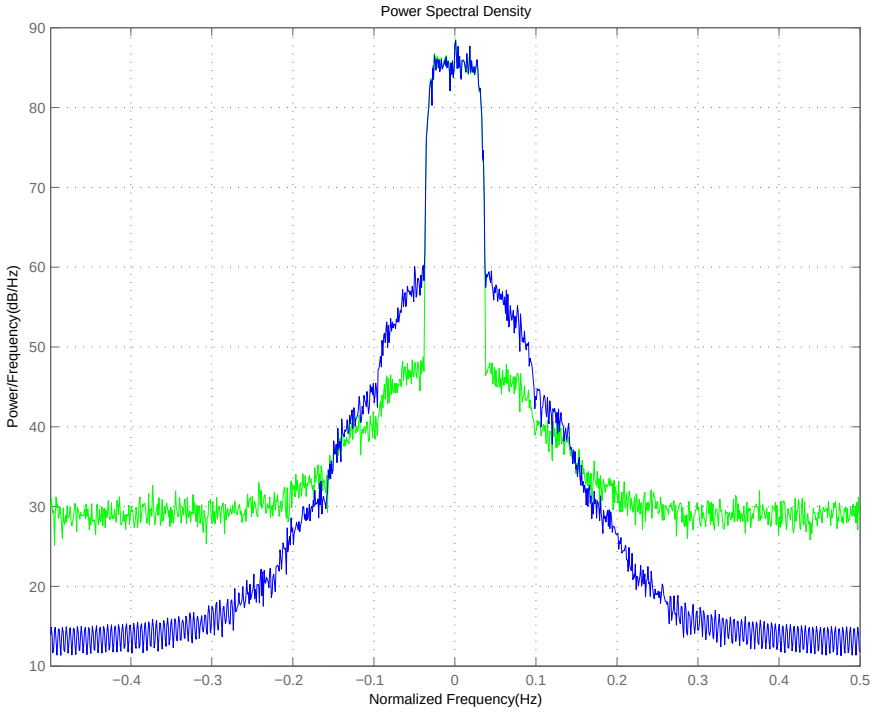

Figure 5.6: Simulated output spectrum with $0.5 * T_s$ delay between input and feedback signals.

in [16] that even if the predistortion on the main path is perfect, the comparator detects a pseudo-error in the case of a small analog delay . Then, the contents of the predistorting signal table are updated by mistake according to the pseudo-errors. Nagata observed that the time delay should be less than 1/64 of a symbol duration. We can conclude that the delay should be made small enough to avoid such an undesirable operation. The result that is obtained is reasonable.

To reduce the improvement decrement, the input and feedback samples are interpolated by a predefined factor to increase the accuracy of time delay estimation. The cross correlation is calculated after the interpolation of the samples, thus 25 dB spectral improvement is maintained even if the delay between the input and the feedback signals has fractional sample time component in it.

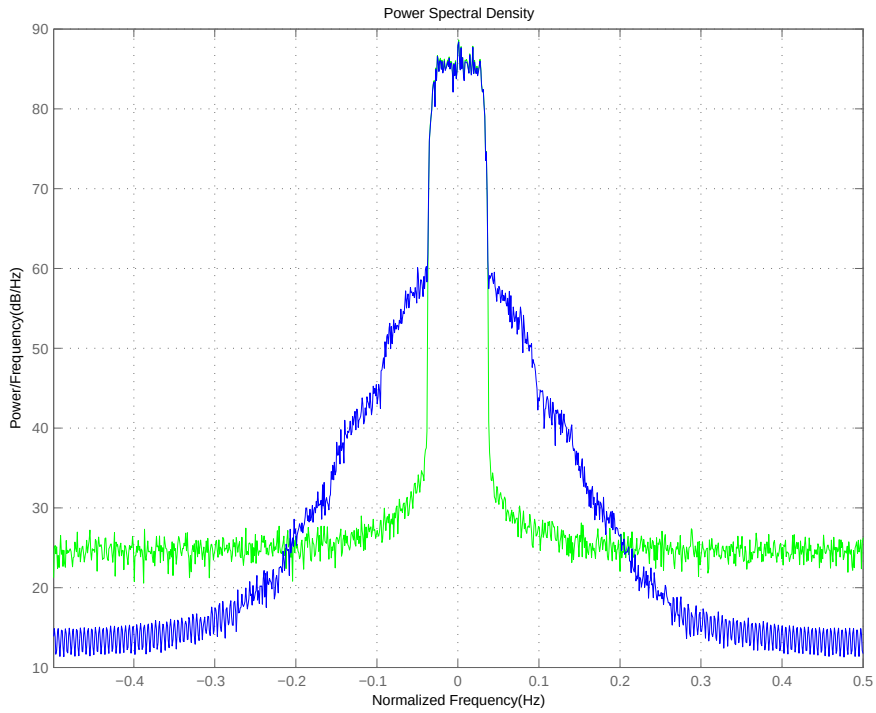

Figure 5.7: Simulated output spectrum with no delay between input and feedback signals.

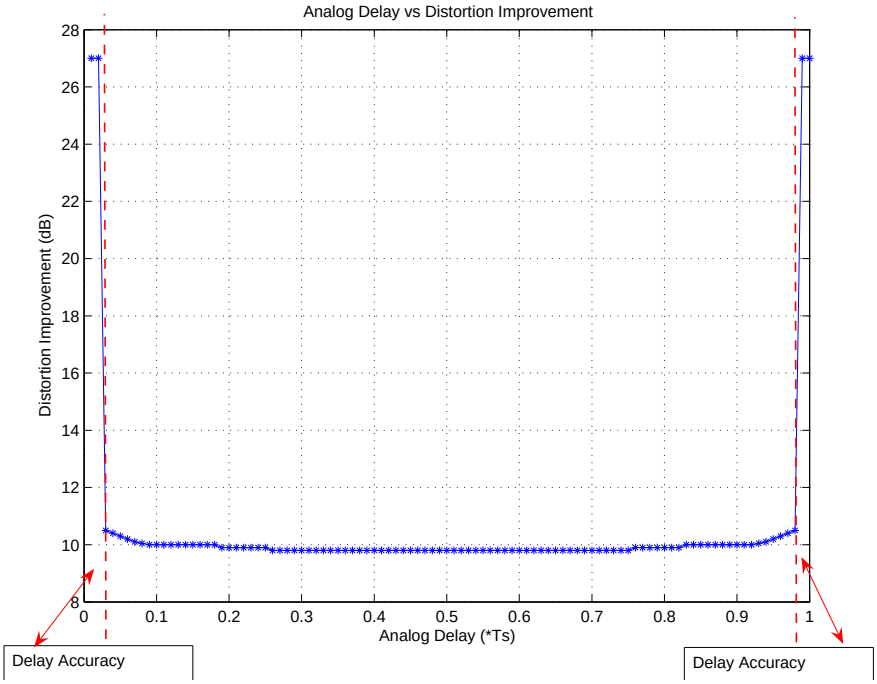

Figure 5.8: Distortion Improvement Sensitivity to Analog Delay

5.5 Response of the Predistorter to Memory Effect

As mentioned in Chapter 2 the memoryless predistorters, which has the adaptation algorithm that depends only on the current value of the input are unsuccessful to compensate for nonlinearity effects of power amplifiers with memory (means that the output of the amplifier at time instant t depends not only on the input at time instant t but also the previous inputs at time instants before t). To observe the response of the predistorter algorithm to memory effect, Nonlinear Tapped Delay Line Memory Model described in 3.3.2.3 is used. The used NTDL model is a 3-tap $5th$ order polynomial presented in Figure 5.9.

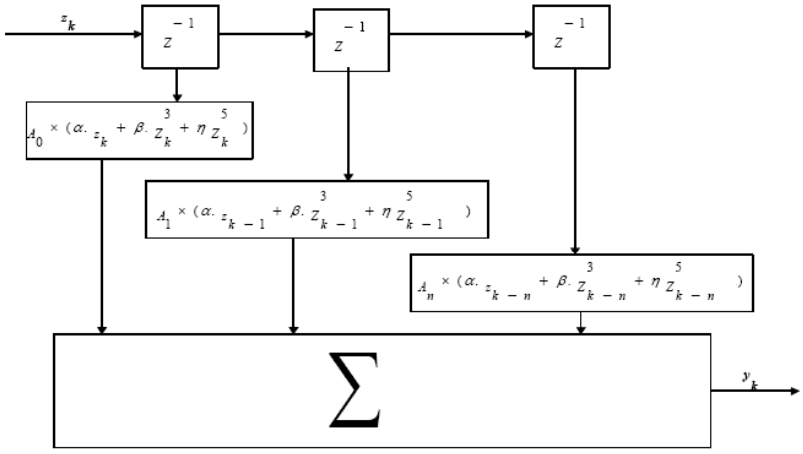

Figure 5.9: The proposed NDTL Power Amplifier Model

The following Figure 5.10 shows the performance of the memoryless predistorter with NDTL power amplifier model. The asymmetry in the power spectrum of the NDTL power amplifier output due to the memory effect can be seen in the figure. The figure 5.10 indicates that it is difficult to cancel the distortion component of power amplifier with memory using predistortion without memory.

One possible way of increasing the improvement again, is to use more than one LUT that is addressed by the magnitude square of the previous input samples. The same adaptation method is used for the other LUTs, but the adaptation

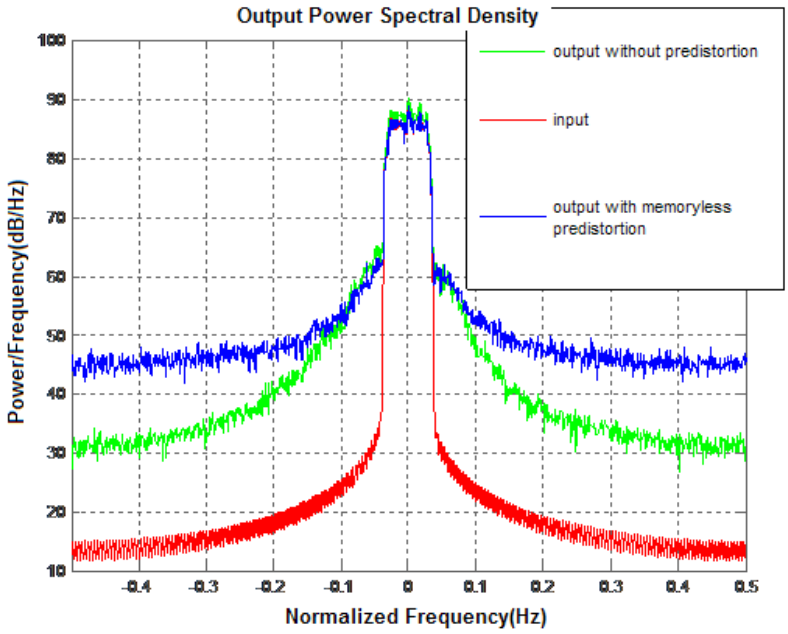

Figure 5.10: Memoryless Predistorter Performance with NTDL Power Amplifier

constant is chosen smaller because following LUTs are wanted to have smaller table entry changes than the previous LUTs has. Figure 5.11 shows the newly used matlab model of the predistorter with memory.

As it is seen in Figure 5.12 we have managed to increase the distortion improvement of 20 dB as compared to the case with memoryless predistorter and amplifier with memory, when two LUTs are used to characterize the memory of the predistorter. Figure 5.13 represents extra 10 dB improvement when three LUTs are used. It is observed that depending on the memory characteristics of the power amplifier, increasing the number of LUTs provides more improvement but requires more space for the LUTs and more convergence time for the adaptation of LUTs's entries.

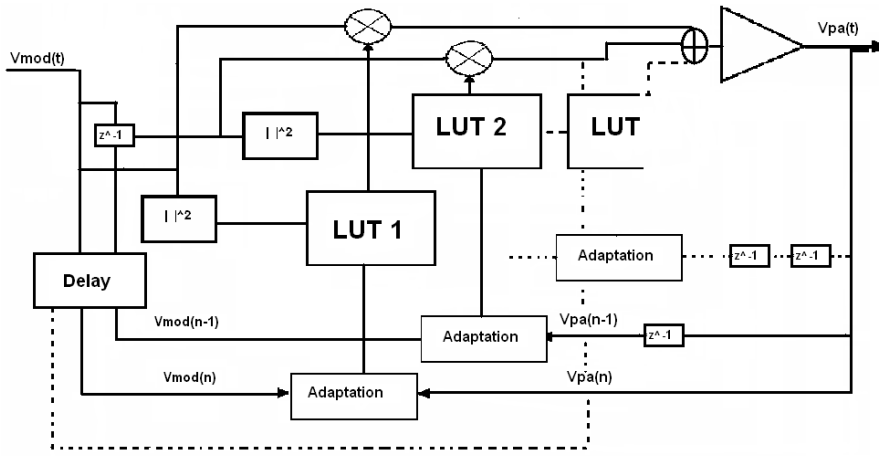

Figure 5.11: Matlab Model of Predistorter with Memory

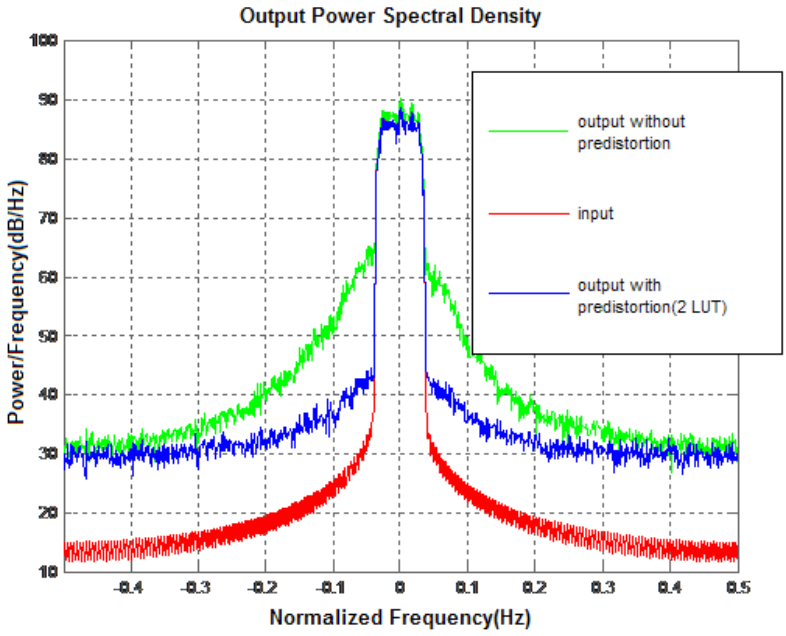

Figure 5.12: Memoryless Predistorter Performance with Power Amplifier with Memory

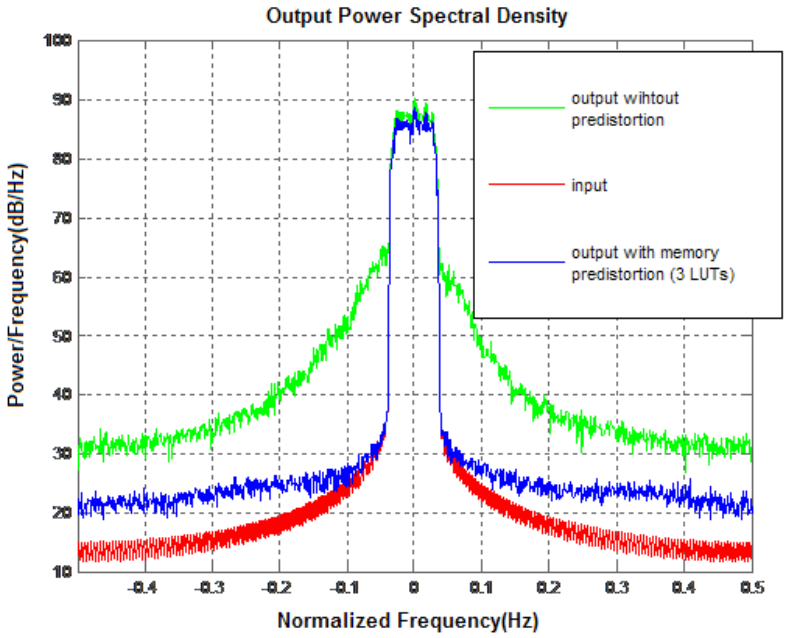

Figure 5.13: Memoryless Predistorter Performance with Power Amplifier with Memory

5.6 Response of the Predistorter to the number of Iteration

As mentioned in chapter 4, the subscript "i" represents a specific entry in the table and k represents the k_{th} iteration of the adaptation algorithm $F_i(k+1) = F_i(k) + \alpha(V_{fb}(t) - V_{mod}(t))(-conj(V_{mod}(t))$. Since the adaptation algorithm is iterative several number of input samples are needed for each entry of the table in order to provide the convergence of the corresponding predistorter complex gain value. The figure 5.6 represents the graph of number of input samples for each entry and corresponding predistorter gain component stored in that entry. It is observed from the figure that at least nine input samples should be addressed to the same entry in order to correctly set the gain component in that entry. As mentioned in section 4.1.5.2, Cavers [3] states that each table entry needs about ten iterations for convergence in the secant method. Since the new algorithm needs about nine iterations for convergence and has less computational load, it is efficient is terms of convergence time and computational load compared to the secant method of adaptation.

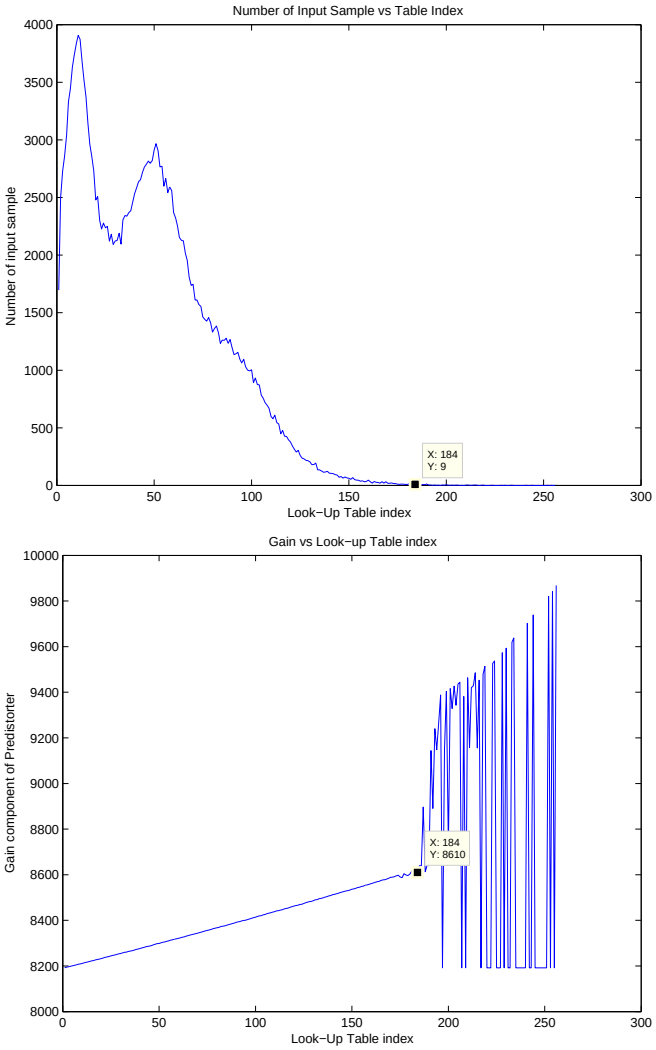

Figure 5.14: Response of the Predistorter without memory to the number of iteration

As it is mentioned in the previous section, if the amplifier has memory and predistortion with memory is used for the elimination of distortion components, adaptation time increases. The number input samples should be addressed to the same entry in order to correctly set the gain component in that entry increases as well. It is observed from figure 5.6 that at least twenty four input samples are needed for the convergence of the corresponding LUT entry gain component.

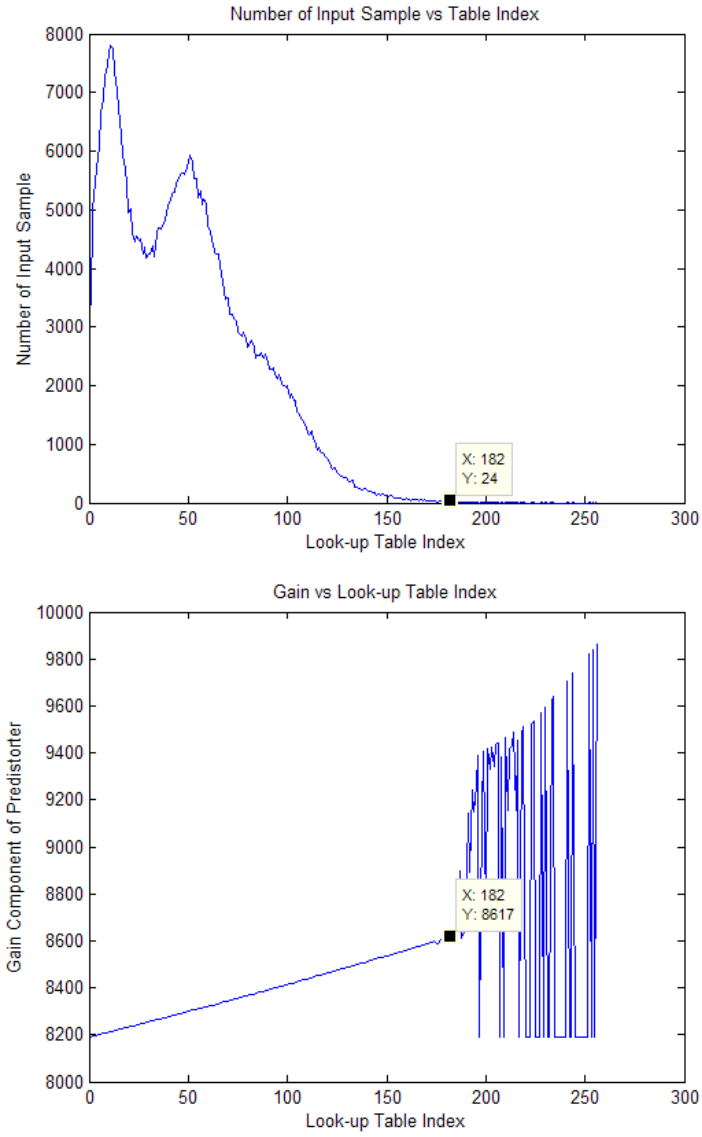

Figure 5.15: Response of the Predistorter with Memory to the number of iteration

Chapter 6

IMPLEMENTATION in SYSTEM GENERATOR and FPGA BOARD

6.1 System Generator Model

The system generator model is used to demonstrate the proposed digital predistortion method. The Xilinx System Generator for DSP is a plug-in to Simulink that enables designers to develop high-performance DSP systems for Xilinx FPGAs. Designers can design and simulate a system using MATLAB, Simulink, and Xilinx library of bit/cycle-true models. The tool will then automatically generate synthesizable Hardware Description Language (HDL) code mapped to Xilinx pre-optimized algorithms. As a result, the system generator is used for design verification upon real time implementation. Figure 6.1 shows the system generator model. The SIMULINK model consisted of three major blocks: QAM signal generation, predistorter (which has address generation, delay adjustment, complex multiplier blocks in it), PA non linearity.

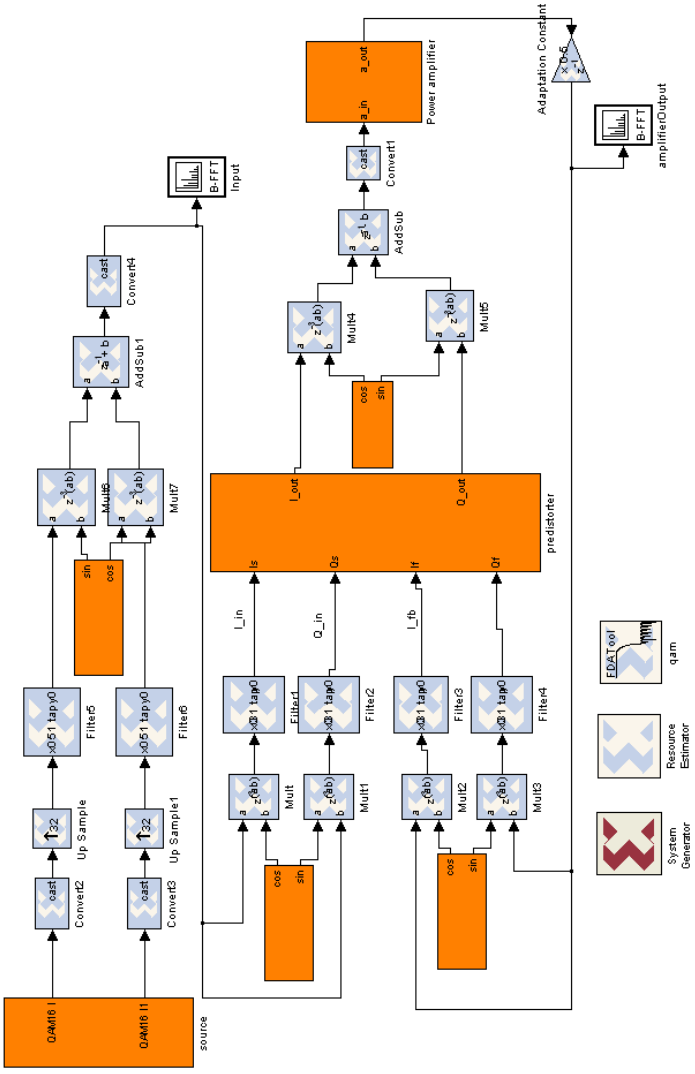

Figure 6.1: System Generator Model

The signal generation block can be programmed to generate any number of adjustable power complex tones. The complex tones are fed to the predistorter block. The address generator block in predistorter block computes the magnitude square of the complex waveform and scales it to address the specified size of the adaptation look-up table. The delay adjust block delays the complex waveform for the required number of samples so that the time alignment between the input complex tones and power amplifier (PA) distorted output complex tones is achieved. The complex multiplier block multiplies the input complex tones with the complex gain values stored in the look-up tables. Therefore predistorting the input to the power amplifier so as to cancel the distortion generated by the power amplifier. The adaptation tables consist of a RAM addressed by the magnitude of the complex input tones and supplies correction vectors to the complex multipliers which pre-distorts the complex input tones fed to the PA. Figure 6.2 shows the power amplifier output spectrum of system generator model with and without predistorter. The spectrum improvement shown in figure 6.2 is obtained when the adaptation constant α is equal to 0.5 and the LUT is addressed by the most significant eighth bits of the calculated magnitude square of the input.

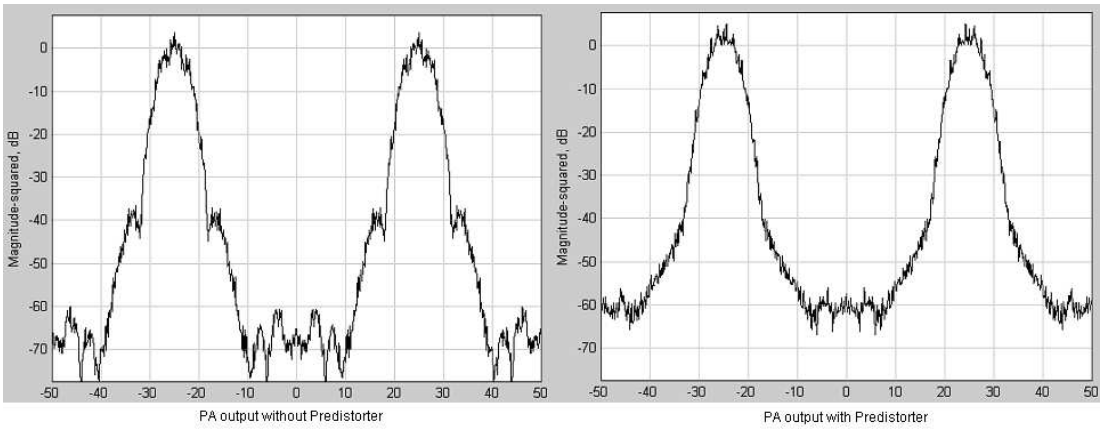

Figure 6.2: Output Power Spectrum of System Generator Model

6.2 FPGA Implementation

We have implemented the algorithm on a modern FPGA chip. Figure 6.3 shows the block diagram of the implemented system. D/A converter connected to the FPGA operated with a speed of 100M samples/second. The constructed FPGA system worked also at the same speed.The used modulation scheme is 16-APSK (Amplitude and Phase Shift Keying). The performance of the system is as predicted in Matlab simulations.

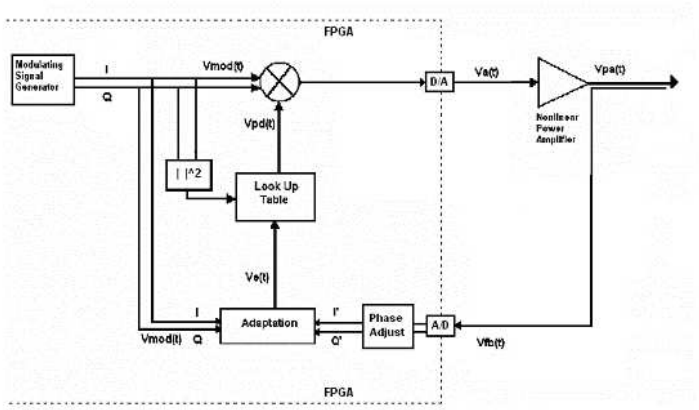

Figure 6.3: Block diagram of the system as implemented on a modern FPGA chip

Output spectral density of the power amplifier is measured before the digital predistortion is turned on. Figure 6.4 shows the spectrum analyzer display of the Vfb signal (downconverted power amplifier output) for a table size of 64. Obviously, there is a great IM3 distortion as observed in the spectrum display.

Figure 6.5 shows the spectrum when the digital predistortion is turned on. The algorithm converges very rapidly and an improvement in neighboring channels is obtained. We note that there is degradation in the background level of the signal due to the small look-up-table size.

The predistorter presented here, provides power efficiency as well as spectral efficiency. As it is mentioned in chapter 5 to improve the background noise level larger size of LUT should be used.

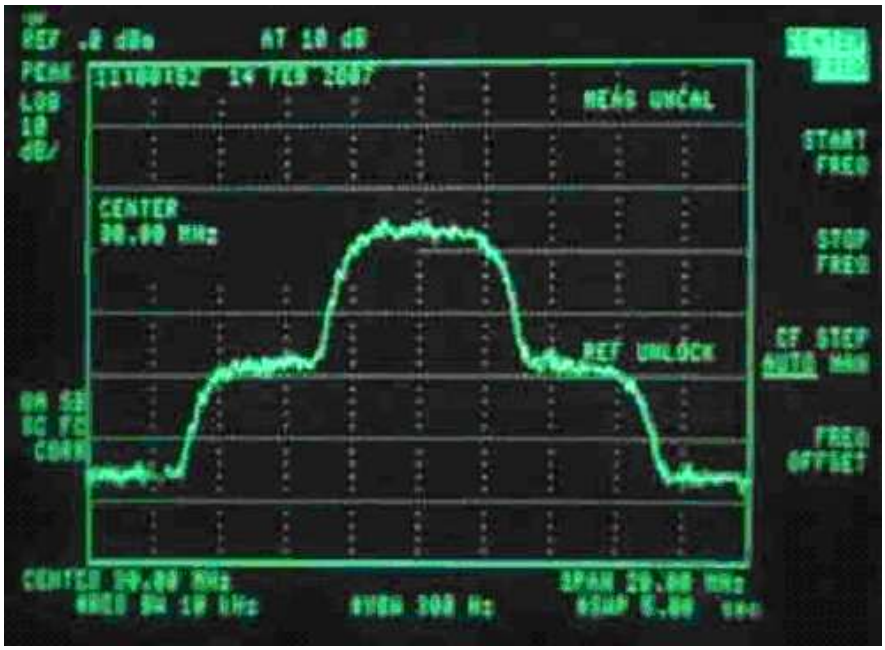

Figure 6.4: Spectrum Analyzer Display of the Power Amplifier Output without Predistortion

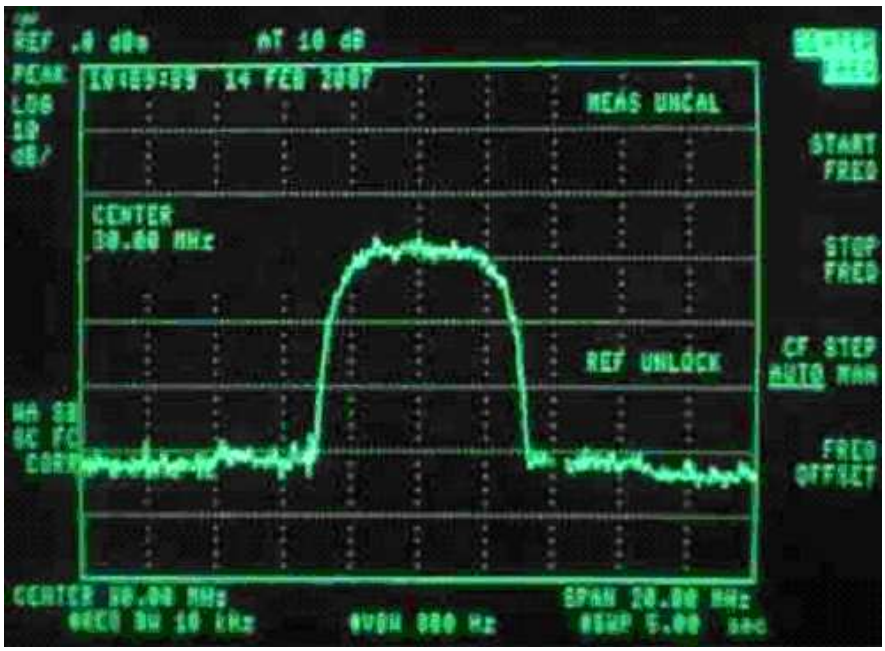

Figure 6.5: Spectrum Analyzer Display of the Power Amplifier Output with Predistortion

Chapter 7

CONCLUSION AND FUTURE WORK

The survey of the common linearization techniques shows that the adaptive digital predistortion method was the most suitable in terms of bandwidth, correction achievable, weight and complexity for the proposed power amplifier architecture.

In this thesis, an adaptive complex gain based look-up table predistorter was implemented and tested. The implementation was done by using Matlab and Simulink Communications Blockset, Signal Processing Blockset and Memoryless Nonlinearity Blockset and System Generator Xilinx Blockset. The testing of the predistorter is done by using a baseband system model which consists of a 16-QAM modulator, an upsampler, a raised cosine filter, the predistorter and a baseband behavioral amplifier model. The amplifier model used is SALEH model. The details of the simulated model was described in chapter 4. It is shown with Matlab simulations that to obtain up to 25-30 dB improvement in power spectrum is possible.

Response analysis of the predistorter parameters presented in chapter 5 shows that the adaptation constant α should be around 0.5. If α is large then the table entries may not converge, but oscillate and result in an unstable system. If α is small then the adaptation time gets longer and with less number of iteration we

may get worse distortion improvement. Response to the table addressing analysis shows that power method of addressing (the magnitude square of the source signal addressing) provides better output power spectrum than linear method of addressing (the magnitude of the source signal addressing) since power method of addressing causes low amplitude coarse. Response to table size analysis shows that increasing the table size reduces the size of discontinuities and hence the background level, but inevitably increases the adaptation time. Response to delay alignment analysis shows that to maintain sufficient linearity improvement the alignment should be within $\frac{1}{80}$ of sample period, otherwise the improvement in power spectrum drops to around 10dB. The performance of the algorithm with an NTDL amplifier model that has memory is also investigated. As expected the improvement decreases. A new method of increasing the improvement again, is to use more than one LUT that is addressed by the magnitude square of the previous input samples and is adapted by the same adaptation algorithm. It is observed that the distortion improvement of extra 25 dB as compared to memoryless predistorter is possible.

System generator model is used for design verification upon real time implementation. By considering all possible real time implementation effects such as bit representations, signs etc. The system generator model results show that the algorithm manages to decrease IM3 products and causes background noise level depending on the table size. We have implemented the algorithms on a modern FPGA chip. D/A converter connected to the FPGA operated with a speed of 100M samples/second. The used modulation scheme is 16-APSK (Amplitude and Phase Shift Keying). The performance of the system is as predicted in Matlab simulations. Close to 20dB IM3 improvement is achieved. As a conclusion,the predistorter presented in this thesis provides power efficiency as well as spectral efficiency. As an advantage it has a simple adaptation algorithm and its complexity is less, therefore it is easy to implement.

Future work related to this thesis can be at first, developing the algorithm such that its sensitivity to analog time mismatch decreases and the background noise level occurred with small LUT size also decreases. Another possible future work is the detailed analysis of FPGA implementation. The figure 7.1 represents

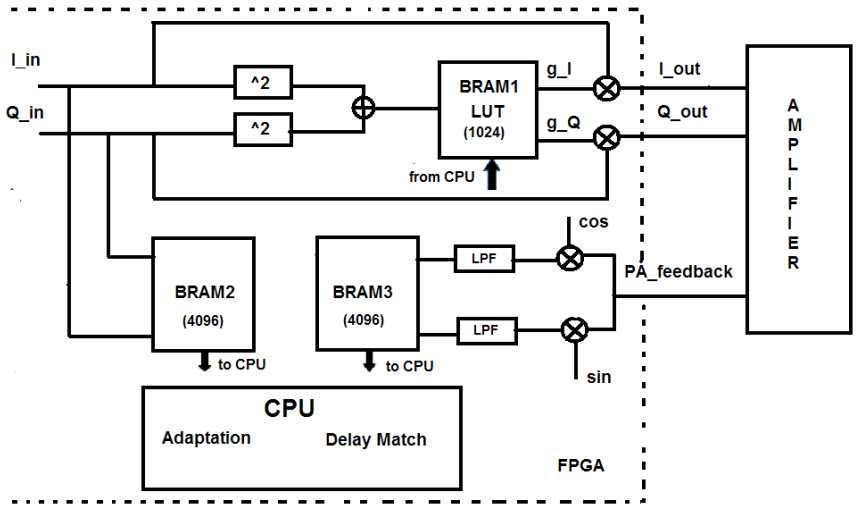

Figure 7.1: The FPGA model as future work

the planned new FPGA model implementation.

Bibliography

[1] T. Arthanake and T. Wood. Linear Amplification using Envelope Feedback. *IEE Electronics Letters*, 31:2023–2024, 1995.

[2] J. S. Cardinal and F. M. Ghannouchi. A new Adaptive Double Envelope Feedback (ADEF) Linearizer for Solid State Power Amplifier. *IEEE Transactions on Microwave Theory and Techniques*, 43:1508 1515, 1995.

[3] J. K. Cavers. A Linearizing Predistorter with Fast Adaptation. *in Proc. IEEE 40th Vehicular Tech. Conf., Orlando, FL*, 45:4147, 1990.

[4] J. K. Cavers. Amplifier Linearization by Adaptive Predistortion. *U.S. Patent 5 049 832*, 1991.

[5] K. Y. Chan and A. Bateman. Analytical and Measured Performance of Combined Analogue Locked Loop Universal Modulator (CALLUM). *IEE Proc-Commun.*, 142:297–306, 1995.

[6] S. C. Cripps. *RF Power Amplifiers for Wireless Communications*. Artech House, Inc., Norwood, MA, USA, 2006.

[7] L. Ding, G. T. Zhou, and R. Raviv. A Hammerstein Predistorter Linearization Design Based on the Indirect Learning Architecture. *Proc. IEEE International Conference on Acoustics, Speech, and Signal Processing*, 3:2689–2692, 2002.

[8] S. A. Hetzel, A. Bateman, and J. P. Mcgeehan. LINC Transmitter. *Electronic Letters*, 27:133–137, 1991.

[9] W. G. Jeon, K. H. Chang, and Y. S. Cho. An Adaptive Data Predistorter for Compensation of Nonlinear Distortion in OFDM systems. *IEEE Transactions on Communications*, 45:11671171, 1997.

[10] M. Johansson and L. Sundström. Linerisation of RF Multicarrier Amplifier using Cartesian Feedback. *Electronics Letters*, 30:1110 1112, 1994.

[11] P. B. Kenington. High Linearity RF Amplifier Design. *Norwood, MA:Artech House*, 2000.

[12] P. B. Kenington and D. W. Bennett. Linear Distortion Correction using a Feedforward System. *IEEE Transactions on Vehicular Technology*, 45:474–480, 1996.

[13] L. Khan. Single-sided Transmission by Envelope Elimination and Restoration. *Proceedings of the IRE*, 40:803–806, 1952.

[14] R. Marsalek. Power Amplifier Linearization using Digital Baseband Adaptive Predistortion, 2003.

[15] K. Miehle. A New Linearization Method for Cancellation of Third Order Distortion. *Masters thesis, The University of North Carolina at Charlotte,Charlotte*, 2003.

[16] Y. Nagata. Linear Amplification Technique for Digital Mobile Communications. *in Proc. IEEE* 39^{th} *Vehicular Tech. Conf.*, 1:159164, 1989.

[17] M. A. Nizamuddin, P. J. Balister, W. H. Tranter, and J. H. Reed. Nonlinear Tapped Delay Line Digital Predistorter for Power Amplifiers with Memory. *Wireless Communications and Networking, 2003. WCNC 2003. 2003 IEEE*, 1:607–611, 2003.

[18] T. Ogunfunmi and S. Chang. Second-order Adaptive Volterra System Identification Based on Discrete Nonlinear Wiener Model. *IEE Proc-Vis. Image Signal Process.*, 148:21–29, 2001.

[19] J. Patel. Adaptive Digital Predistortion Linearizer for Power Amplifiers in Military UHF Satellite. *College of Engineering University of South Florida*, 2004.

[20] V. Petrovic and W. Gosling. Polar Loop Transmitter, 1979.

[21] F. H. Raab. L-band Transmitter using Kahn EER Technique. *IEEE Trans. Microwave Theory Tech.*, 46:22202225, 1998.

[22] T. S. Rappaport. *Wireless Communications: Principles and Practice (2nd Edition)*. Prentice Hall PTR, December 2001.

[23] B. Şekerlisoy and S. Köse. Adaptive Digital Predistortion. *Senior Project Design, Bilkent University*, 2005.

[24] D. K. Su and W. J. McFarland. An IC for Linearizing RF Power Amplifier using Envelope Elimination and Restoration. *IEEE Journal of Solid-State Circuits*, 33:2252–2258, 1998.

[25] L. Sundström. Digital RF Power Amplifier Linearisers Analysis and Design, 1995.

[26] L. Sundström. The Effects of Quantization in Digital Signal Component Separator for LINC Transmitter. *IEEE Transactions on Vehicular Technology*, 45:346–352, 1996.

[27] P. Wambacq and W. Sansen. Distortion Analysis of Analog Integrated Circuits. *MA: Kluwer*, 1998.

[28] A. Zhu, M. Wren, and T. J. Brazil. An Adaptive Volterra Predistorter for the Linearization of RF Power Amplifiers. *IEEE MTT-S Digest*, 2002.